Multifaceted modes of γ-tubulin complex recruitment and microtubule nucleation at mitotic centrosomes

Zihan Zhu[1], Corinne A. Tovey[2], Eugenie C. Yen[1], Fred Bernard[2], Antoine Guichet[2], and Paul T. Conduit[1,2,3]

[1]Department of Zoology, University of Cambridge, Downing Street, Cambridge, CB2 3EJ

[2]Université Paris Cité, CNRS, Institut Jacques Monod, F-75013 Paris, France.

[3]Corresponding author
Paul T. Conduit
Institut Jacques Monod
CNRS - Université Paris Cité
15 rue Hélène Brion
75013 Paris
France
0033 (1) 57 27 80 95
paul.conduit@ijm.fr
ORCID: 0000-0002-7822-1191

Keywords: Centrosome, γ-tubulin, γ-TuRC, microtubule, Drosophila.

Summary

Microtubule nucleation is catalysed by multi-protein γ-tubulin ring complexes (γ-TuRCs). In most eukaryotes, a GCP4/5/4/6 “core” complex promotes γ-tubulin small complex (γ-TuSC) association to generate γ-TuRCs within the cytosol. However, the importance of this core complex is uncertain, as its components are non-essential in various species. In *Drosophila*, Spindle defective-2 (Spd-2) and Centrosomin (Cnn) redundantly recruit γ-tubulin complexes to centrosomes during mitosis, but it remains unclear how. Here we show that Spd-2 recruits γ-TuRCs formed via the GCP4/5/4/6 core, but that Cnn can recruit γ-TuSCs independently of the GCP4/5/4/6 core via its well-conserved CM1 domain. Moreover, by selectively abolishing γ-tubulin complex recruitment, we show that mitotic centrosomes can nucleate microtubules independently of γ-tubulin complexes and that this depends on the TOG domain protein Mini-spindles (Msps). Collectively, our data help explain the dispensability of the GCP4/5/4/6 core for *Drosophila* development and show why centrosomes are such robust microtubule organising centres.

Introduction

During cell division, centrosomes act as major microtubule organising centres (MTOCs) to nucleate and organise microtubules that form the mitotic spindle (Conduit et al., 2015). Centrosomes comprise a pair of centrioles that recruit and are surrounded by the pericentriolar material (PCM). The PCM is a large collection of proteins that includes γ-tubulin ring complexes (γ-TuRCs) and is the predominant site of microtubule nucleation and organisation. On entry into mitosis, centrosomes expand their PCM to increase their potential to nucleate and organise microtubules, in a process called centrosome maturation (Khodjakov and Rieder, 1999; Piehl et al., 2004). Centrosome maturation is particularly dramatic in *Drosophila* cells because interphase centrosomes have very little PCM and do not organise microtubules, while mitotic centrosomes have relatively large amounts of PCM and robustly organise microtubules (Rogers et al., 2008). This makes *Drosophila* centrosomes ideal for the study of PCM assembly and microtubule nucleation.

γ-tubulin complexes are important PCM clients, as they template and catalyse microtubule nucleation (Tovey and Conduit, 2018; Farache et al., 2018; Kollman et al., 2011). They comprise a single-turn helical arrangement of 14 laterally associated "spokes", each made from a γ-tubulin complex protein (GCP, or "Grip" protein in *Drosophila*) and a γ-tubulin molecule. The essential subunits of γ-TuRCs are 2-spoke γ-tubulin small complexes (γ-TuSCs), made from GCP2, GCP3 and two γ-tubulins. In budding yeast, only γ-TuSCs are present and they are stimulated to assemble into helical structures when bound by the conserved "Centrosomin motif 1" (CM1) domain found within the yeast spindle pole body (SPB; centrosome equivalent) proteins Spd110 and Spc72 (Stu2, a TOG domain protein, is also required in the case of Spc72) (Kollman et al., 2010; Gunzelmann et al., 2018a). The "CM1 motif" within Spc110's CM1 domain binds across adjacent γ-TuSCs, which presumably promotes the oligomerisation process at the SPB (Brilot et al., 2021; Lyon et al., 2016; Kollman et al., 2010; Lin et al., 2014). In most eukaryotes, however, γ-TuSCs are stimulated to assemble into γ-TuRCs within the cytosol via a 4-spoke GCP4/5/4/6 core complex that seeds ring assembly (Haren et al., 2020; Würtz et al., 2022). Indeed, depletion of GCP4, GCP5 or GCP6 strongly inhibits cytosolic γ-TuRC assembly in human,

Xenopus, *Drosophila*, *Aspergillus*, and fission yeast cells (Cota et al., 2017; Vogt et al., 2006; Vérollet et al., 2006; Xiong and Oakley, 2009; Zhang et al., 2000). Intriguingly, however, these γ-TuRC-specific proteins are not essential in *Drosophila*, *Aspergillus*, or fission yeast (Xiong and Oakley, 2009; Vogt et al., 2006; Anders et al., 2006; Vérollet et al., 2006). Consistent with this, γ-TuSCs can be recruited to *Drosophila* S2 cell centrosomes after depletion of core components (Vérollet et al., 2006), and are recruited independently of the core components to the outer SPB plaque in *Aspergillus* (Gao et al., 2019). Nevertheless, how γ-TuSCs are recruited to centrosomes in the absence of the GCP4/5/4/6 core remains unclear.

The predominant view of γ-tubulin complex recruitment involves the binding of large coiled-coil "tethering proteins" whose experimental depletion leads to measurable reductions in γ-tubulin levels at centrosomes. One of these proteins, NEDD1/Grip71, associates with pre-formed γ-TuRCs in the cytosol and subsequently docks γ-TuRCs to centrosomes (Lüders et al., 2006; Haren et al., 2006, 2009; Zhang et al., 2009; Gomez-Ferreria et al., 2012a; b). All other tethering proteins do not associate with cytosolic γ-TuRCs but instead localise to centrosomes and appear to "dock" incoming γ-tubulin complexes. These include the Pericentrin family of proteins, proteins containing the conserved CM1 domain (e.g. human CDK5RAP2, *Drosophila* Centrosomin (Cnn), fission yeast Mto1, and budding yeast Spc110 and Spc72), and the Spd-2 family of proteins (CEP192 in humans) (Zimmerman et al., 2004; Gomez-Ferreria et al., 2007; Haren et al., 2009; Fong et al., 2008; Sawin et al., 2004; Zhang and Megraw, 2007; Conduit et al., 2014; Dobbelaere et al., 2008; Lee and Rhee, 2011). It is complicated to interpret the individual role of these proteins in the recruitment of γ-tubulin complexes, however, as they depend upon each other for their proper localisation within the PCM and act redundantly. We previously showed that γ-tubulin could accumulate at mitotic centrosomes in the absence of either Cnn or Spd-2, but fails to accumulate when both proteins are removed, with centrosomes also failing to accumulate other PCM proteins and failing to nucleate microtubules (Conduit et al., 2014). Cnn and Spd-2 can therefore both independently recruit γ-tubulin complexes to mitotic centrosomes, but how they do so remains unknown.

Cnn contains the highly conserved CM1 domain (Sawin et al., 2004), which binds directly to γ-tubulin complexes in yeast and humans (Brilot et al., 2021; Wieczorek et al., 2019) and has been implicated in the recruitment of γ-tubulin complexes to centrosomes in different systems (Zhang and Megraw, 2007; Lyon et al., 2016; Samejima et al., 2008; Choi et al., 2010; Muroyama et al., 2016; Fong et al., 2008). The importance of the CM1 domain in *Drosophila* Cnn is less clear, however, because its removal reduces, but does not abolish, γ-tubulin accumulation at mitotic centrosomes (Zhang and Megraw, 2007). This could be due to the presence of Spd-2, but this has not been tested. In contrast to Cnn, Spd-2 does not contain a CM1 domain and so how it recruits γ-tubulin complexes remains to be established.

In this study, we investigated how γ-tubulin complexes are recruited to mitotic centrosomes by Cnn and Spd-2. We used classical *Drosophila* genetics to combine specific mutant alleles or RNAi constructs and examined γ-tubulin recruitment in larval brain cells. We show that Cnn can recruit γ-tubulin in the absence of the GPC4/5/4/6 core and Grip71 and that this is dependent on its CM1 domain. This suggests that Cnn can recruit γ-TuSCs to centrosomes via its CM1 domain, similar to Spc110 and Spc72 in budding yeast. In contrast, we find that Spd-2 fails to recruit γ-tubulin in the absence of the GPC4/5/4/6 core and Grip71, showing that recruitment via Spd-2 requires γ-TuRCs to pre-form in the cytosol. In addition, we show that mitotic centrosomes can still nucleate and organise microtubules in the total absence of γ-tubulin complexes. We found that this γ-tubulin-independent mode of microtubule nucleation relies on the *Drosophila* TOG domain protein Minispindles (Msps), consistent with the conserved ability of TOG domain proteins to catalyse microtubule nucleation *in vitro*. Our data provide an explanation for how γ-TuSCs are recruited to centrosomes in the absence of the GPC4/5/4/6 core, and highlight the robustness of centrosomes to recruit γ-tubulin complexes and nucleate microtubules.

Results

Cnn recruits γ-tubulin complexes via its CM1 domain independently of Grip71 and the GCP4/5/4/6 core

We first explored how Cnn recruits γ-tubulin complexes to mitotic centrosomes by comparing the levels of centrosomal γ-tubulin at interphase and mitotic centrosomes in larval brain cells from flies lacking Spd-2 and different γ-tubulin complex proteins. Typically, interphase centrosomes have only ~5-20% of the γ-tubulin levels found at mitotic centrosomes, and this residual γ-tubulin is closely associated with the centrioles and is non-functional with respect to microtubule nucleation. An increase in γ-tubulin signal between interphase and mitotic centrosomes indicates that γ-tubulin complexes have been recruited to the expanding mitotic PCM, at least to some degree. Similar to our previous results (Conduit et al., 2014), we found that γ-tubulin was recruited to mitotic centrosomes in *spd-2* mutant brains with an average level of ~77% compared to wild-type brains (Figure 1A,B; note that each point in Figure 1B corresponds to the average centrosomal signal from a single brain and not just to a single centrosome). We know that this recruitment of γ-tubulin is entirely dependent on Cnn, because centrosomes in *cnn,spd2* double mutants fail entirely to recruit γ-tubulin during mitosis (Conduit et al., 2014). In contrast to combining *spd-2* mutant alleles with *cnn* mutant alleles, however, combining *spd-2* mutant alleles with mutant or RNAi alleles for Grip71 and the GCP4/5/4/6 core components did not prevent γ-tubulin accumulation at mitotic centrosomes. In fact, the centrosomes in these *spd-2,grip71,grip75*^{GCP4}*,grip128*^{GCP5}-RNAi,*grip163*^{GCP6} mutant cells had ~66% of the γ-tubulin levels found at wild-type centrosomes, similar to the levels found at *spd-2* mutants alone (Figure 1A,B). Thus, the recruitment of γ-tubulin to mitotic centrosomes that occurs in the absence of Spd-2, i.e. that depends upon Cnn, does not require Grip71 or the GCP4/5/4/6 core. Given that the GCP4/5/4/6 core complex is required for cytosolic γ-TuRC assembly, our data show that Cnn can recruit γ-TuSCs directly from the cytosol.

The recruitment of γ-TuSCs to centrosomes by Cnn appears to reflect the natural situation in budding yeast, where γ-TuSCs are recruited to the SPB by the CM1 domain proteins Spc110 and Spc72. We therefore reasoned that Cnn's recruitment of γ-TuSCs should be also be mediated by its CM1 domain. A previous study, however, had shown that replacing the endogenous *cnn* gene with an ectopically expressed UAS-GFP-Cnn construct lacking the CM1 domain led to a reduction, but not elimination, of γ-tubulin at centrosomes in syncytial embryos (Zhang and Megraw, 2007). Along with the potential effects caused by Cnn over-expression, we now know that Spd-2 can recruit γ-tubulin complexes independently of Cnn (Conduit et al., 2014), making it hard to evaluate the true effect of deleting the CM1 domain without first removing Spd-2. We therefore used CRISPR combined with homology-directed repair to delete the CM1 domain (amino acids 98-167) from the endogenous *cnn* gene and combined this allele with the *spd-2* mutant allele. We found that γ-tubulin no longer accumulated at mitotic centrosomes in these $cnn^{\Delta CM1}$,*spd-2* mutant cells (Figure 1C,D), showing definitively that Cnn's CM1 domain is essential for Cnn to recruit γ-tubulin complexes to mitotic centrosomes.

We also tested whether the CM1 domain was required for Cnn to bind γ-tubulin complexes by comparing the ability of bacterially purified MBP-tagged Cnn fragments to bind and co-immunoprecipitate γ-tubulin from cytosolic embryo extracts. We recently showed that Cnn's centrosomal isoform (Cnn-C) is auto-inhibited from binding cytosolic γ-tubulin complexes by an extreme N-terminal "CM1 auto-inhibition" (CAI) domain, but that this auto-inhibition can be relieved by introducing T27E and S186D phospho-mimetic mutations (Tovey et al., 2021). These mutations were therefore included in the fragments to enable Cnn binding in control conditions (Cnn-C-$N^{T27E,S186D}$). To identify mutations predicted to perturb CM1 binding, we used cross-species protein sequence alignments and identified F115, R101, and E102 as equivalent to residues important for γ-tubulin complex binding in humans (F75) (Choi et al., 2010) and budding yeast (K120 and E121) (Lin et al., 2014; Gunzelmann et al., 2018b) (Figure 1E). We mutated these residues in the Cnn-C-$N^{T27E,S186D}$ fragments to R101Q, E102A and F115A to mimic the mutations previously used in yeast and human

experiments (Cnn-C-N^{T27E,S186D,R101Q,E102A,F115A}). Strikingly, these three point mutations in the CM1 motif region (R101Q/E102A/F115A) completely abolished the ability of the phospho-mimicked MBP-Cnn fragments to co-immunoprecipitate γ-tubulin (Figure 1F), showing that Cnn's CM1 domain is required for binding to γ-tubulin complexes.

Taken together, our data show that Cnn can mediate the recruitment of γ-tubulin complexes to mitotic centrosomes in the absence of Grip71 and the GCP4/5/4/6 core and that this depends on its CM1 domain. This indicates that, similar to Spc110 and Spc72 in budding yeast, *Drosophila* Cnn can bind and recruit γ-TuSCs to centrosomes without requiring γ-TuRCs to first form within the cytosol.

Spd-2 predominantly recruits pre-formed γ-TuRCs from the cytosol

To explore how Spd-2 recruits γ-tubulin complexes even though (unlike Cnn) it lacks a CM1 domain, we compared the levels of centrosomal γ-tubulin at interphase and mitotic centrosomes in larval brain cells from flies lacking Cnn and different γ-tubulin complex proteins. Cnn is essential to maintain high levels of Spd-2 within the PCM, and so mitotic centrosomes in a *cnn* mutant background recruit only ~22% of γ-tubulin compared to wild-type cells (Conduit et al., 2014). We were therefore testing which γ-TuRC components, when removed, reduced this level further, such that there was no significant accumulation of γ-tubulin between interphase and mitotic centrosomes. Note also that centrioles are frequently offset from the centre of the PCM in *cnn* mutants (Lucas and Raff, 2007), resulting in the centriole signal appearing on the edge of the γ-tubulin signal (Figure 2A). We predicted that Spd-2 recruits γ-tubulin complexes via Grip71, because the human homologue of Spd-2, Cep192, associates with the human homologue of Grip71, NEDD1 (Gomez-Ferreria et al., 2012a). We found, however, that γ-tubulin could still accumulate at mitotic centrosomes relatively well in *cnn,grip71* mutant cells, reaching ~15% the levels of wild-type cells (Figure 2A,B). This means that Spd-2's ability to recruit γ-tubulin complexes relies only partly on Grip71. There was a stronger reduction, however, when we removed Cnn and members of the GCP4/5/4/6 core, Grip75^{GCP4} and Grip163^{GCP6}, either individually or in combination (Figure 2A,B). Given that the GCP4/5/4/6 core is required for the

assembly of γ-TuRCs within the cytosol, this result suggests that Spd-2 (unlike Cnn) predominantly recruits pre-formed γ-TuRCs rather than γ-TuSCs. We found, however, that the accumulation of γ-tubulin at mitotic centrosomes was only completely abolished after the additional removal of Grip71 i.e. in *cnn,grip71,grip163*^{GCP6} mutant cells (Figure 2A,B), a phenotype that was not due to a failure of Spd-2 to accumulate at mitotic centrosomes (Figure 2C,D). Thus, Spd-2 can recruit a very small amount of γ-TuSCs via Grip71 (i.e. the recruitment that occurs in cnn,grip75^{GCP4},grip163 ^{GCP6} cells), but its recruitment of γ-tubulin complexes relies predominantly on the GCP4/5/4/6 core.

Intriguingly, γ-tubulin could still accumulate at mitotic centrosomes to some degree in cells lacking Cnn, Grip71 and Grip75^{GCP4}, showing that removal of Grip75^{GCP4} does not perfectly phenocopy the removal of Grip163^{GCP6}, and therefore suggesting that Grip163^{GCP6} may still be able to promote γ-TuRC assembly to some degree in the absence of Grip75^{GCP4}. This is consistent with observations in human cells, where GCP6 depletion has a greater effect on cytosolic γ-TuRC assembly than GCP4 depletion (Cota et al., 2017). Alternatively, Spd-2 may interact with γ-tubulin complexes specifically via Grip163^{GCP6} and the residual γ-tubulin we see at mitotic centrosomes in *cnn,grip71,grip75*^{GCP4} mutant cells may reflect the recruitment of Grip163^{GCP} and its associated γ-tubulin. In summary, Spd-2's recruitment of γ-TuRCs relies strongly on the presence of the GCP4/5/4/6 core, although removal of Grip71, as well as the GCP4/5/4/6 core, are both required to entirely prevent accumulation of γ-tubulin at mitotic centrosomes.

Collectively, our data show that Spd-2's recruitment of γ-tubulin complexes relies almost entirely on the GCP4/5/4/6 core, and therefore on γ-TuRC assembly within the cytosol, but that Cnn's conserved CM1 domain can mediate the recruitment of γ-TuSCs (Figure 2E). The requirement of Spd-2 for the GCP4/5/4/6 core reflects the fact that homologues of the GCP4/5/4/6 core and Spd-2 are not encoded in lower eukaryotes. In addition, the ability of Cnn to recruit γ-TuSCs may explain why the GCP4/5/4/6 core is not essential in several species studied so far, particularly if all

CM1 domain proteins are able to stimulate γ-TuSC assembly into ring-like structures, as is the case for yeast Spc110 and Spc72.

Centrosomes lacking γ-tubulin can still nucleate and organise microtubules

In the course of examining *cnn,grip71,grip163* mutants, we observed that their mitotic centrosomes, which fail to accumulate γ-tubulin but still accumulate Spd-2, were still associated with microtubules during prophase and localised to spindle poles during mitosis (Figure 3A). This is in contrast to centrosomes in *cnn,spd-2* mutant cells which lack PCM entirely and fail to nucleate or organise microtubules (Conduit et al., 2014). This suggested that mitotic centrosomes could be sites of γ-TuRC-independent microtubule nucleation events so long as the PCM could still assemble to some extent. To test whether the microtubules associated with *cnn,grip71,grip163* mutant centrosomes (hereafter, "γ-tubulin-negative" centrosomes) were actually nucleated at centrosomes (rather than being nucleated elsewhere and then attaching to the centrosomes) we performed a cooling-warming microtubule repolymerisation assay. We depolymerised microtubules by cooling larval brains on ice for ~40 minutes and then either chemically fixed samples on ice or allowed them to warm up for 30 seconds before rapid chemical fixation. ~40 minutes of cooling efficiently depolymerised microtubules at most centrosomes (Figure 3B). After 30s warming, all wild-type and γ-tubulin-negative centrosomes had an associated α-tubulin signal, either as asters or as part of a re-formed mitotic spindle (Figure 3C). Thus, mitotic centrosomes in *Drosophila* appear to be able to nucleate microtubules in the absence of γ-tubulin complexes.

To better understand microtubule dynamics at wild-type and γ-tubulin-negative centrosomes we established a system to image cells live while cooling and warming the sample. We generated stocks containing fluorescent markers of microtubules (Jupiter-mCherry) and centrosomes (GFP-PACT) with and without the *cnn*, *grip71* and *grip163* mutations and used a microscope-fitted heating-cooling device (CherryTemp) to modulate the temperature of larval brain samples during recording. We imaged samples for ~30s before cooling them to 5˚C for 3 minutes to depolymerise microtubules and then rapidly warming them to 20˚C to observe microtubule regrowth.

When cells were cooled to 5˚C, the centrosomal Jupiter-mCherry signal decreased towards cytosolic background levels at both control and γ-tubulin-negative centrosomes (Figure 3D-F; Videos S1 and S2). In a subset of cells, this centrosomal signal reached cytosolic levels (i.e. disappeared) after 3 minutes of cooling (Figure S2A,B). On warming to 20˚C, there was an immediate increase in the centrosomal Jupiter-mCherry signal at all control and γ-tubulin-negative centrosomes (Figure 3D-F; Figure S2A,B), confirming that microtubules can be nucleated at centrosomes lacking γ-tubulin.

While microtubules could be nucleated at centrosomes in *cnn,grip71,grip163* mutant cells, plotting the mean Jupiter-mCherry signal through time revealed that the dynamics of microtubules at these γ-tubulin-negative centrosomes different to those at control centrosomes (Figure 3F). On cooling to 5˚C, microtubules depolymerised faster at control centrosomes (Figure 3F), which was best seen when plotting the depolymerisation phases and fitting "one-phase exponential decay" models (R^2 = 0.995 and 0.987 for control and γ-tubulin-negative centrosomes, respectively) (Figure 3G). This showed that the Jupiter-mCherry signal at control and γ-tubulin-negative centrosomes had a half-life of 21.79 and 44.88 seconds, respectively, and decay rate constants of 0.0361 and 0.0154, respectively. On warming to 20˚C, microtubules also polymerised faster at control centrosomes (Figure 3F). Fitting "exponential plateau" models (R^2 = 0.999 and R^2 = 0.994 for control and γ-tubulin-negative centrosomes, respectively) showed that the growth rate constants were 0.0759 and 0.0536, respectively (Figure 3H). Thus, microtubules depolymerise faster and then are nucleated and/or polymerise faster at control centrosomes compared to at γ-tubulin-negative centrosomes.

These differences in microtubule dynamics between control and γ-tubulin-negative centrosomes were also apparent when imaging EB1-GFP comets, which mark growing microtubule plus ends, during cooling-warming cycles. EB1-GFP comets emerging from control centrosomes disappeared immediately after cooling to 5˚C and then reappeared immediately after warming to 20˚C (Figure 3I; Video S3). In contrast, EB1-GFP comets emerging from γ-tubulin-negative centrosomes took longer to

disappear after cooling, and fewer comets reappeared after warming (Figure 3J; Video S4). Moreover, it was easier to observe EB1-GFP comets emerging from chromatin regions in these *cnn,grip71;grip163* mutant cells (Figure 3J; Video S4), presumably because the centrosomes were no longer such dominant sites of microtubule nucleation.

Our data suggest that microtubules are more resistant to cold-induced depolymerisation when they have been nucleated independently of γ-TuRCs, but that microtubules are nucleated more efficiently when γ-TuRCs are present. However, it must be considered that, due to the loss of Cnn from centrosomes in the *cnn,grip71,grip163* mutant cells, general PCM levels are reduced, likely reducing the levels of any protein involved in γ-TuRC-independent microtubule nucleation. Nevertheless, our data clearly shows that microtubules can be nucleated independently of γ-TuRCs from mitotic centrosomes in *Drosophila*.

<u>The TOG domain protein Msps promotes microtubule nucleation from centrosomes lacking γ-tubulin complexes</u>

We next addressed which proteins promote γ-TuRC-independent microtubule nucleation at mitotic centrosomes. We did not observe any clear enrichment of α-tubulin at centrosomes after microtubule depolymerisation (Figure 3B; Figure S1), ruling out the possibility that a high local concentration of α/β-tubulin accounts for or contributes to γ-TuRC-independent microtubule nucleation. Proteins of the TOG domain and TPX2 protein families are often reported to promote γ-TuRC-independent microtubule nucleation. These proteins promote microtubule nucleation in a range of species both *in vitro* and *in vivo*, including in the absence of γ-TuRCs (see Discussion and references therein). The *Drosophila* TOG domain protein homologue is Minispindles (Msps). Msps binds microtubules, localises to centrosomes and spindle microtubules and is required for proper spindle formation, mitotic progression and chromosome segregation (Cullen et al., 1999). Msps has been reported to stabilise the minus ends of microtubules when bound and recruited to centrosomes by TACC (Barros et al., 2005; Lee et al., 2001). Msps is also part of a group of proteins that organise microtubules independently of γ-tubulin at the nuclear envelope of fat body

cells (Zheng et al., 2020). Moreover, the TOG1 and 2 domains of Msps promote microtubule nucleation *in vitro* (Slep and Vale, 2007). The putative *Drosophila* TPX2 homologue is Mei-38 and, while its depletion results in only mild spindle defects, Mei-38 binds microtubules, localises to centrosomes and spindle microtubules, and is required for microtubule re-growth from kinetochores (Popova et al., 2022; Goshima, 2011). CAMSAP/Patronin/Nezha protein family members have also been implicated in γ-TuRC-independent microtubule nucleation and organisation at non-centrosomal sites (Akhmanova and Kapitein, 2022) and CAMSAP2 condensates can stimulate microtubule nucleation *in vitro* (Imasaki et al., 2022).

To test the role of these proteins in γ-TuRC-independent nucleation from centrosomes, we combined mutant or RNAi alleles with the *cnn*, *grip71*, and *grip163* mutant alleles and analysed microtubule organisation at centrosomes during prophase, when microtubule asters are most robust (Conduit et al., 2014). We were unable to obtain 3rd instar lavae when combining the *cnn*, *grip71*, and *grip163* mutant alleles with *patronin* mutant or RNAi alleles, presumably due to severe microtubule defects that prevented development. We could therefore not test the role of Patronin, although we note that we did not readily observe Patronin-GFP at centrosomes in larval brain cells (data not shown). We could, however, obtain larvae when combining the *cnn*, *grip71*, and *grip163* mutant alleles with mutant alleles for *msps* or *tacc* or an RNAi allele for Mei38. Clear association of microtubules with centrosomes was observed in 100% of wild-type prophase cells and in 96.8% of *cnn,grip71,grip163* mutant prophase cells (Figure 4A,B,F), consistent with our observations above that the γ-tubulin-negative centrosomes in *cnn,grip71,grip163* mutant cells can nucleate microtubules. In contrast, a clear association of microtubules with centrosomes was observed in only 55.3% of *cnn,grip71,grip163,msps* mutant prophase cells, and in 70.7% and 81.4% of *cnn,grip71,grip163,tacc* and *cnn,grip71,grip163,mei-38-RNAi* mutant cells, respectively (Figure 4C-F). Moreover, the γ-tubulin/msps-negative centrosomes within *cnn,grip71,grip163,msps* mutant cells tended to be positioned further from the spindle poles than the γ-tubulin-negative centrosomes within *cnn,grip71,grip163* mutant cells (Figure 4G,H), which is indicative of a reduced capacity to organise microtubules. Positioning of centrosomes in

cnn,grip71,grip163,tacc and *cnn,grip71,grip163,mei-38-RNAi* mutant cells was less affected, reflecting the less severe defects in microtubule organisation at γ-tubulin/Tacc-negative and γ-tubulin/Mei38-negative centrosomes.

Given that Msps appeared to be most important for γ-TuRC-independent nucleation of microtubules from centrosomes, we tested its role directly by performing a cooling/warming microtubule nucleation assay (similar to the fixed cell assay performed in Figure 3B,C) and compared the recovery of microtubules 30 seconds post warming at γ-tubulin-negative centrosomes within *cnn,grip71,grip163* mutant cells and at γ-tubulin/msps-negative centrosomes in *cnn,grip71,grip163,msps* mutant cells. We categorised cells as those with or without centrosomes (some cells lack centrosomes due to mis-segregation of centrosomes during mitosis) and those that had or had not yet formed spindles; the proportion of these categories was similar in both mutant types (Figure S3). There were, however, differences between the mutant types within each category. Of the cells that contained centrosomes but had not yet formed a spindle, γ-tubulin-negative centrosomes organised microtubules in ~94.3% of *cnn,grip71,grip163* mutant cells, the majority of which were scored as having strong or medium asters, but γ-tubulin/msps-negative centrosomes organised microtubules in only ~37.7% of *cnn,grip71,grip163,msps* mutant cells, the majority of which were scored as having weak asters (Figure 5A,B). This difference appeared to affect spindle formation because, of the cells that had centrosomes and that had formed a spindle structure, spindles were scored as being of “high” or “medium” quality (based on their morphology and density) in ~67.1% of *cnn,grip71,grip163* mutant cells but in only ~28% of *cnn,grip71,grip163,msps* mutant cells (Figure 5C,D). This was specific to centrosomes because there was a similarly high proportion of cells containing low quality spindles in both mutant types when cells lacked centrosomes (Figure 5E).

In summary, our data show that centrosomes lacking γ-tubulin complexes can still nucleate microtubules, despite having reduced PCM, and that the TOG domain protein Msps plays an important role in this γ-TuRC-independent microtubule nucleation pathway.

Discussion

How centrosomes nucleate and organise microtubules is a long-standing question. Centrosomes contain hundreds of proteins, many of which associate with microtubules, meaning that understanding how centrosomes nucleate and organise microtubules is not trivial. Prior to our current work, we had identified Cnn and Spd-2 as the two key PCM components in flies – remove one and the other could support partial PCM assembly and microtubule organisation; remove both and PCM assembly and microtubule organisation fail (Conduit et al., 2014). We had found that γ-tubulin could still accumulate at mitotic centrosomes after removal of either Cnn or Spd-2, showing that both proteins could mediate the recruitment of γ-tubulin complexes, but it remained unclear how. The work presented here shows that Cnn and Spd-2 recruit different types of γ-tubulin complex, with Cnn able to recruit γ-TuSCs and Spd-2 recruiting predominantly pre-formed γ-TuRCs. Moreover, by preventing γ-tubulin recruitment but not PCM assembly, we have shown that centrosomes still nucleate microtubules in the absence of γ-TuRCs and that this γ-TuRC-independent mode of microtubule nucleation is stimulated by the TOG domain protein Msps.

By using classical genetics, we have found that Cnn can recruit γ-tubulin complexes independently of Grip71 and the GCP4/5/4/6 core, meaning that it must be able to recruit γ-TuSCs. This is consistent with previous observations showing that γ-TuSCs could still be recruited to mitotic *Drosophila* centrosomes in S2 cells lacking the GCP4/5/4/6 core components (Vogt et al., 2006), although it was unknown at that time that this recruitment was dependent on Cnn. Our data here also shows that this occurs *in vivo*. The ability of Cnn to recruit γ-TuSCs is similar to its budding yeast homologues' ability, where Grip71 and the GCP4/5/4/6 core are naturally absent. Consistent with this, we show that Cnn's binding and recruitment of γ-tubulin complexes relies entirely on its highly conserved CM1 domain, which binds across the inter γ-TuSC interface in budding yeast complexes (Brilot et al., 2021). The binding of the CM1 domain in budding yeast stimulates the oligomerisation of γ-TuSCs into γ-TuRCs (Kollman et al., 2010; Lyon et al., 2016; Brilot et al., 2021; Lin et al., 2014; Gunzelmann et al., 2018a), but whether this is true of Cnn's CM1 domain, or CM1 domains in other eukaryotes, remains to be determined. Cnn's CM1 domain is more similar to Spc110's CM1

domain than to Spc72's CM1 domain, which requires the TOG domain protein Stu2 for efficient oligomerisation of γ-TuSCs, suggesting that Cnn may have this ability. Consistent with this possibility, Grip71 and the GCP4/5/4/6 core components are not essential in flies (Reschen et al., 2012; Vogt et al., 2006), nor in *Aspergillus* or *S. pombe* (Xiong and Oakley, 2009; Anders et al., 2006), suggesting that there must be ways to assemble ring-like templates in these organisms in the absence of the GCP4/5/4/6 core. We speculate that this "other way" is via CM1-mediated oligomerisation of γ-TuSCs. Nevertheless, Cnn and other CM1 domain proteins can also bind γ-TuRCs formed via the GCP4/5/4/6 core (Muroyama et al., 2016; Choi et al., 2010; Tovey et al., 2021; Wieczorek et al., 2020, 2019) and so it remains unclear whether Cnn recruits γ-TuSCs only in the absence of pre-formed γ-TuRCs.

In contrast to Cnn, Spd-2 (which does not contain a CM1 domain) requires Grip71 and the GCP4/5/4/6 core to recruit γ-tubulin complexes to mitotic centrosomes i.e. it is unable to bind and recruit γ-TuSCs directly or mediate their recruitment by another protein. Whether Spd-2 binds directly to preformed γ-TuRCs remains unclear. Grip71 associates with pre-formed γ-TuRCs in the cytosol and the human homologue of Grip71, NEDD1, has been reported to interact with the human homologue of Spd-2, CEP192 (Gomez-Ferreria et al., 2012a). Thus, Spd-2 might recruit γ-TuRCs via binding to Grip71, but since we show that Spd-2 can recruit γ-TuRCs in the absence of Grip71, it must also be able to recruit γ-TuRCs in a different way. Our data show that Grip163^{GCP6} is more important than Grip75^{GCP4} for Spd-2's recruitment of γ-TuRCs, because removing Grip71 and Grip75^{GCP4} does not completely abolish γ-tubulin accumulation. This may suggest that Spd-2 recruits γ-TuRCs via an interaction with Grip163^{GCP6}, or simply that Grip163^{GCP6}, but not Grip75^{GCP4}, is essential for the assembly of pre-formed γ-TuRCs necessary for Spd-2-mediated recruitment. This would be consistent with findings in human cells, where depletion of GCP6 is more disruptive to γ-TuRC assembly than depletion of GCP4 (Cota et al., 2017). So far, our attempts to identify direct interactions between Spd-2 and γ-TuRC components have failed, and so it is possible that an intermediary protein links Spd-2 to γ-TuRCs.

The finding that Cnn and Spd-2 recruit different types of γ-tubulin complexes to centrosomes fits well with recent observations that not all γ-TuRCs within a given species or cell type have the same protein composition. This was shown by analysing the γ-TuRC protein Mozart1 (Mzt1) in *Drosophila*, *C. elegans*, fission yeast and *Aspergillus*, where Mzt1 is either not present or not necessary at certain MTOCs (Tovey et al., 2018; Gao et al., 2019; Huang et al., 2020; Sallee et al., 2018). For example, we have shown that *Drosophila* Mzt1 is expressed only in developing sperm cells and is required for γ-TuRC recruitment to basal bodies but not mitochondria (Tovey et al., 2018). Moreover, in mouse epithelial cells γ-TuRCs are bound and recruited either by CDK5RAP2 (Cnn homologue) or by NEDD1 (Grip71 homologue) and this influences the nucleation and anchoring ability of the γ-TuRCs (Muroyama et al., 2016). Whether even more forms of γ-TuRCs exist and how this affects their function remains to be explored.

In addition to revealing details of γ-tubulin complex recruitment to centrosomes, we have also shown that microtubules can be nucleated from centrosomes in the absence of γ-tubulin complexes. It is has been known for some time that microtubules can still be observed within cells after depletion of γ-tubulin or other key γ-TuRC proteins (Hannak et al., 2002; Strome et al., 2001; Sampaio et al., 2001; Sunkel et al., 1995; Tsuchiya and Goshima, 2021; Sallee et al., 2018; Rogers et al., 2008; Nakaoka et al., 2015; Wang et al., 2015; Gunzelmann et al., 2018b) and that certain non-centrosomal MTOCs naturally lack γ-tubulin (Nashchekin et al., 2016; Yang and Wildonger, 2020; Zheng et al., 2020; Mukherjee et al., 2020; Kitamura et al., 2010). Mounting evidence, including our work here, suggests that the ch-Tog/XMAP215/Msps/Alp14/Stu2 TOG domain family of proteins (which have microtubule polymerase activity) and the TPX2 family of proteins (which have microtubule stabilization activity) are important for microtubule nucleation. Depletion of TOG domain proteins from *Xenopus* egg extracts, *Drosophila* S2 and fat body cells, fission yeast cells, and budding yeast cells, and depletion of TPX2 from *Xenopus* egg extracts, severely impairs microtubule nucleation or organisation (Popov et al., 2002; Thawani et al., 2018; Zheng et al., 2020; Groen et al., 2009; Flor-Parra et al., 2018; Gunzelmann et al., 2018b). TOG domain and TPX2 proteins have been shown to work together with γ-TuRCs (or microtubule seed

templates) to promote microtubule nucleation (Thawani et al., 2018; Flor-Parra et al., 2018; Gunzelmann et al., 2018b; Consolati et al., 2020; King et al., 2020; Wieczorek et al., 2015), but studies, mainly *in vitro*, have shown that they can also function independently of γ-TuRCs to promote microtubule nucleation (Roostalu et al., 2015; Woodruff et al., 2017; Schatz et al., 2003; Slep and Vale, 2007; Ghosh et al., 2013; Thawani et al., 2018; King et al., 2020; Zheng et al., 2020; Tsuchiya and Goshima, 2021; Imasaki et al., 2022). Our data suggest that the *Drosophila* TOG domain protein Msps promotes γ-TuRC-independent microtubule nucleation from mitotic centrosomes. This finding is similar to that of a recent study in human colon cancer cells showing that γ-tubulin depletion did not prevent microtubule nucleation from centrosomes and that this γ-TuRC-independent microtubule nucleation pathway depended on the Msps homologue ch-TOG (Tsuchiya and Goshima, 2021), and supports the observation that *C. elegans* centrosome-like condensates formed *in vitro* nucleate microtubules with help from the TOG domain protein Zyg-9 (Woodruff et al., 2017). It is possible that Patronin is also involved in γ-TuRC-independent microtubule nucleation from centrosomes, but we were unable to test this due to developmental arrest when combining mutant or RNAi alleles for *patronin*. We note, however, that we could not readily detect Patronin-GFP at centrosomes in dividing larval brain cells (data not shown). In flies at least, the γ-TuRC-independent mode of microtubule nucleation at centrosomes does not appear to rely on a localised increase in the concentration of tubulin, as in *C. elegans* (Woodruff et al., 2017; Baumgart et al., 2019), because we did not observe α-tubulin concentrating at centrosomes after microtubule depolymerisation.

So why are γ-TuRCs required at all? While microtubules can be nucleated independently of γ-TuRCs, nucleation appears to be more efficient when γ-TuRCs are present ((Tsuchiya and Goshima, 2021; Hannak et al., 2002);this study). Naturally occurring γ-TuRC-independent microtubule nucleation at specialised MTOCs, such as the nuclear envelope of *Drosophila* fat body cells (Zheng et al., 2020), may not require a high frequency of microtubule nucleation events, perhaps because they build their microtubule arrays over a relatively long period of time. During cell division, however, many microtubules must be generated rapidly, possibly creating a

requirement for γ-TuRCs to provide efficient microtubule nucleation. Indeed, depleting γ-TuRCs delays spindle assembly and results in spindle and chromosome defects (Sunkel et al., 1995; Sampaio et al., 2001; Colombié et al., 2006; Vérollet et al., 2006). γ-TuRCs may also be important to set microtubule protofilament number and define microtubule polarity, and studies have implicated γ-tubulin or γ-TuRC proteins in the control microtubule dynamics and of cell cycle progression, independent of their microtubule nucleation roles (Oakley et al., 2015; Bouissou et al., 2009).

In summary, our data highlight the robustness of centrosomes to nucleate microtubules. We have shown that centrosomes can recruit different forms of γ-tubulin complexes (γ-TuSCs and γ-TuRCs) via multiple pathways and that they can nucleate and organise microtubules in the absence of γ-tubulin complexes. This γ-TuRC-independent mode of microtubule nucleation relies on the TOG domain protein Msps. This multi-pathway redundancy helps explain why centrosomes are such dominant MTOCs during mitosis.

Methods

Transgenic and endogenously modified *Drosophila* lines

The Jupiter-mCherry (Callan et al., 2010), GFP-PACT (Martinez-Campos et al., 2004) and RFP-PACT (Conduit et al., 2010) alleles have been described previously. To delete the CM1 domain from Cnn, we first designed a pCFD4 vector (Port et al., 2014) containing two guide RNAs with the following target sequences: AACTCGCCCTTGCCGTCACA and GTGATGAGAAATGGCTCGAG. This vector was injected into flies containing the attP2 landing site by Rainbow Transgenic Flies, Inc. Camarillo, CA 93012, USA. Male flies were then crossed to females expressing nos-cas9 (BL54591) and the resultant embryos were injected by the Department of Genetics Fly facility, University of Cambridge, UK, with a homology vector encoding 1kb on either side of the deletion region (R98 to D167). The resulting F0 flies were crossed to balancer lines and their progeny were screened by PCR for the deletion.

The endogenously-tagged EB1-GFP line was made using CRISPR-based genome editing by inDroso, France. An SSSS-eGFP-3'UTR-LoxP-3xP3-dsRED-LoxP cassette was inserted and then the selection markers were excised. The guide RNA sequences were not communicated and the company has now closed.

Fly Stocks

The following mutant alleles were used to examine brains cells lacking specific proteins: for γ-tubulin: *γ-tubulin23C*$^{A15-2}$/*γ-tubulin23C*^{df}; Cnn: *cnn*^{f04547}/*cnn*^{HK21}; for Spd-2: *dspd-2*^{Z35711}/*dspd-2*$^{Df(3L)st-j7}$: for Grip71: *grip71*^{120}/*grip71*^{df6041}; for Grip75: *grip75*^{175}/*Grip75*^{df7048}; for Grip163: *grip163*^{GE2708}*; grip163*^{df6115}. For RNAi of *grip128* or *mei-38*: *grip128*-RNAi^{V29074} and *mei-38*-RNAi^{HMJ23752}, respectively, together with Insc-Gal4 (BL8751). RNAi was used for these genes as their position on the X chromosome made generating stocks with multiple alleles technically challenging. Moreover, the only available mutant of *mei*-38 affects a neighbouring gene. For examining the behaviour of MTs in living larval brain cells, we analysed brains expressing 2 copies of Ubq-GFP-PACT and 2 copies of Ubq-Jupiter-mCherry in either a WT or a

cnn,grip71,grip163 mutant background. For examining the behaviour of EB1-GFP in living larval brain cells, we analysed brains expressing 2 copies of EB1-GFP in either a WT or a *cnn,grip71,grip163* mutant background.

Antibodies

For immunofluorescence analysis, we used the following antibodies: mouse anti-γ-tubulin monoclonal (1:500; GTU88, Sigma), mouse anti-α-tubulin monoclonal (1:1000; DM1α, Sigma), rabbit anti-α-tubulin monoclonal (1:500; AB52866, Abcam), anti-PhosphoHistoneH3 monoclonal (mouse, 1:2000, Abcam or rabbit, 1:500, Cell Signalling Technology), Guinea pig anti-Asl polyclonal (1:500; Gift from Jordan Raff), rabbit anti-DSpd-2 polyclonal (1:500) (Dix and Raff, 2007). Secondary antibodies were from Molecular Probes (Invitrogen): Alexa Fluor 488, 568, and 647 (all used at 1:1000). For western blotting we used mouse anti-γ-tubulin monoclonal (1:250; GTU88, Sigma) and rabbit anti-MBP polyclonal (1:1000; gift from Jordan Raff).

Fixed brain analysis

For the analysis of centrosomal fluorescence levels of γ-tubulin or other PCM components, 3rd instar larval brains were processed as described previously (Conduit et al., 2014). Briefly, dissected larval brains were incubated in 100mM colchicine in Schneider's medium for 1h at 25°C to depolymerise microtubules. This prevents centrosomes in *cnn* mutants from "rocketing" and transiently losing their PCM (Lucas and Raff, 2007), allowing a more accurate quantification of PCM recruitment (Conduit et al., 2014). Brains were fixed in 4% paraformaldehyde containing 100mM PIPES, 1mM $MgSO_4$, and 2mM EGTA pH 6.95 for 20 minutes at room temperature, washed in PBS and then 45% and 60% acetic acid, squashed under a coverslip, post-fixed in methanol, washed in PBT, and then stained with the appropriate antibodies. Images were collected on a Leica SP5 point scanning upright confocal system run by LAS AF software using a 63X 1.3NA glycerol objective (Leica 1156194). At least 5 images containing multiple cells in both mitosis (as shown by positive Phospho-Histone H3 staining) and interphase were collected for each brain. Each data point on a graph represents the average signal from all the centrosomes quantified in a single brain.

Typically, between 30 and 50 centrosomes were analysed per cell cycle stage (interphase or mitosis) per brain.

For assessing the ability of centrosomes to organise microtubules during prophase, 3rd instar larval brains were treated and imaged as above except that the colchicine incubation step was omitted. A prophase cell was scored as positive when at least one centrosome had an associated α-tubulin signal. For measuring the distance of centrosomes from the spindle pole during prometaphase, measurements were made between the centre of Asl signal (centrosome) and the spindle pole (centre of the α-tubulin signal at the spindle pole).

Fixed microtubule re-growth assay

3rd instar larval brains of the appropriate genotype were dissected and incubated on ice in Schneider's medium for 40 minutes. Empirical tests showed that a 40-minute incubation was necessary to efficiently depolymerise centrosomal microtubules. Larval brains were then either rapidly fixed on ice in 16% paraformaldehyde containing 100mM PIPES, 1mM $MgSO_4$, and 2mM EGTA pH 6.95 for 5 minutes (T0 brains), or were quickly transferred to room temperature for 30 seconds and then rapidly fixed at room temperature. Subsequently, the brains were processed as above.

Live analysis of microtubule and EB1-GFP comets during cooling warming cycles

A CherryTemp device from CherryBiotech was used to modulate the temperature of larval brain cells. 3rd instar larval brains were dissected and semi-squashed between a coverslip and the CherryTemp thermalisation chip in Schneider's medium and then imaged on a Leica DM IL LED inverted microscope controlled by μManager software and coupled to a RetigaR1 monochrome camera (QImaging) and a CoolLED pE-300 Ultra light source using a 63X 1.3NA oil objective (Leica 11506384). The temperature was changed from 20˚C to 5˚C and back to 20˚C for microtubule depolymerisation and repolymerisation, respectively. Temperature changes induce movements in the glass and the focus was manually adjusted to keep as many frames in focus as possible during the temperature shifts. For Jupiter-mCherry Videos, Z-stacks with gaps of

500nm were acquired every 6 seconds; for EB1-GFP Videos, Z-stacks with gaps of 300nm were acquired every second.

Image analysis and statistics

All images were processed in Fiji (Image J). Each Z-stack image was reconstructed by maximum intensity Z-axis projection. PCM or microtubule levels at centrosomes were calculated by measuring the total fluorescence in a boxed or circular region around the centrosome and subtracting the local cytoplasmic background fluorescence. GraphPad Prism was used for statistical analysis. Details of the statistical tests and models used can be found in the figure legends.

Recombinant protein cloning, expression and purification

The Cnn-C-$N^{T27E,S186D}$ fragment comprises amino acids 1-255 of Cnn-C and was generated previously (Tovey et al., 2021). We generated the Cnn-C-$N^{T27E,R101Q,E102A,F115A,S186D}$ fragment in a similar manner. Briefly, a pDEST-HisMBP (Addgene, #11085) vector containing aa1-255 of Cnn was digested with KpnI and SspI and a complementary fragment containing the point mutations was cloned into the cut vector using HiFi technology (NEB). The complementary fragment was generated by GENEWIZ. The vector was transformed into BL21-DE3 cells and the protein purified using gravity flow amylose resin (New England Biolabs) affinity chromatography. Peak elution fractions were diluted 1:1 with glycerol and stored at -20°C.

Immunoprecipitation and western blotting

Immunoprecipitation was carried out as previously (Tovey et al., 2021). Briefly, 1g/ml of embryos were homogenised in homogenisation buffer containing 50 mM HEPES, pH7.6, 1mM $MgCl_2$, 1 mM EGTA, 50 mM KCl supplemented with PMSF 1:100, Protease Inhibitor Cocktail (1:100, Sigma Aldrich) and DTT (1M, 1:1000). Extracts were clarified by centrifugation twice for 15 minutes at 16,000 rcf at 4°C and 100 µl embryo extract was rotated at 4°C overnight with 30 µl magnetic ProteinA dynabeads (Life Technologies) coupled with anti-MBP antibodies (gift from Jordan Raff) and MBP-Cnn fragments. Beads were washed 5 times for 1 min each in PBS + 0.1% triton (PBST), boiled in 50 µl 2x sample buffer (BioRad), and separated from the eluted IP

sample using a magnet. Samples were analysed by electrophoresis and western blotting as described previously (Tovey et al., 2021). Membranes were imaged using a BioRad ChemiDoc.

Acknowledgements

This research was supported by a Wellcome Trust and Royal Society Sir Henry Dale fellowship awarded to PTC [105653/Z/14/Z], by a Chaire d'excellence grant from the IdEx Université Paris Cité ANR-18-IDEX-0001 awarded to PTC, by an Association pour la Recherche sur le Cancer grant (PJA 20181208148) awarded to AG, and by the CNRS. We thank Jordan Raff for sharing antibodies and fly lines. We thank Corinne Tovey and Roger Karess for their invaluable input and critical reading of the manuscript. The work benefited from the Imaging Facility, Department of Zoology, University of Cambridge, supported by Matt Wayland and a Sir Isaac Newton Trust Research Grant (18.07ii(c)), and from the ImagoSeine at the IJM, Paris. For the purpose of Open Access, the author has applied a CC BY public copyright license to any Author Accepted Manuscript version arising from this submission.

Author Contributions

ZZ produced fly stocks by combining alleles, performed cell imaging experiments, in particular establishing and executing the cooling-warming assays, and analysed data. CT designed and performed the immunoprecipitation experiment, including cloning and protein purification of the Cnn fragments, and provided feedback on the manuscript. EY contributed to establishing the fixed cell cooling-warming experiment. AG obtained funding to generate the EB1-GFP fly line via InDroso with coordination from FB. PTC obtained funding, designed the study, produced fly stocks by combining alleles, performed cell imaging experiments, analysed data, and wrote the manuscript.

References

Akhmanova, A., and L.C. Kapitein. 2022. Mechanisms of microtubule organization in differentiated animal cells. *Nat Rev Mol Cell Bio*. 23:541–558. doi:10.1038/s41580-022-00473-y.

Anders, A., P.C.C. Lourenço, and K.E. Sawin. 2006. Noncore components of the fission yeast gamma-tubulin complex. *Mol Biol Cell*. 17:5075 5093. doi:10.1091/mbc.e05-11-1009.

Barros, T.P., K. Kinoshita, A.A. Hyman, and J.W. Raff. 2005. Aurora A activates D-TACC–Msps complexes exclusively at centrosomes to stabilize centrosomal microtubules. *J Cell Biology*. 170:1039–1046. doi:10.1083/jcb.200504097.

Baumgart, J., M. Kirchner, S. Redemann, A. Bond, J. Woodruff, J.-M. Verbavatz, F. Jülicher, T. Müller-Reichert, A.A. Hyman, and J. Brugués. 2019. Soluble tubulin is significantly enriched at mitotic centrosomes. *J Cell Biol*. 218:3977–3985. doi:10.1083/jcb.201902069.

Bouissou, A., C. Vérollet, A. Sousa, P. Sampaio, M. Wright, C.E. Sunkel, A. Merdes, and B. Raynaud-Messina. 2009. γ-Tubulin ring complexes regulate microtubule plus end dynamics. *J Cell Biology*. 187:327–334. doi:10.1083/jcb.200905060.

Brilot, A.F., A.S. Lyon, A. Zelter, S. Viswanath, A. Maxwell, M.J. MacCoss, E.G. Muller, A. Sali, T.N. Davis, and D.A. Agard. 2021. CM1-driven assembly and activation of yeast γ-tubulin small complex underlies microtubule nucleation. *Elife*. 10:e65168. doi:10.7554/elife.65168.

Callan, M.A., C. Cabernard, J. Heck, S. Luois, C.Q. Doe, and D.C. Zarnescu. 2010. Fragile X protein controls neural stem cell proliferation in the Drosophila brain. *Hum Mol Genet*. 19:3068 3079. doi:10.1093/hmg/ddq213.

Choi, Y.-K., P. Liu, S.K. Sze, C. Dai, and R.Z. Qi. 2010. CDK5RAP2 stimulates microtubule nucleation by the γ-tubulin ring complex. *J Cell Biology*. 191:1089–1095. doi:10.1083/jcb.201007030.

Colombié, N., C. Vérollet, P. Sampaio, A. Moisand, C. Sunkel, H.-M. Bourbon, M. Wright, and B. Raynaud-Messina. 2006. The Drosophila gamma-tubulin small complex subunit Dgrip84 is required for structural and functional integrity of the spindle apparatus. *Mol Biol Cell*. 17:272 282. doi:10.1091/mbc.e05-08-0722.

Conduit, P.T., K. Brunk, J. Dobbelaere, C.I. Dix, E.P. Lucas, and J.W. Raff. 2010. Centrioles regulate centrosome size by controlling the rate of Cnn incorporation into the PCM. *Curr Biol*. 20:2178 2186. doi:10.1016/j.cub.2010.11.011.

Conduit, P.T., J.H. Richens, A. Wainman, J. Holder, C.C. Vicente, M.B. Pratt, C.I. Dix, Z.A. Novak, I.M. Dobbie, L. Schermelleh, and J.W. Raff. 2014. A molecular

mechanism of mitotic centrosome assembly in Drosophila. *Elife*. 3:2987. doi:10.7554/elife.03399.

Conduit, P.T., A. Wainman, and J.W. Raff. 2015. Centrosome function and assembly in animal cells. *Nat Rev Mol Cell Bio*. 16:611 624. doi:10.1038/nrm4062.

Consolati, T., J. Locke, J. Roostalu, Z.A. Chen, J. Gannon, J. Asthana, W.M. Lim, F. Martino, M.A. Cvetkovic, J. Rappsilber, A. Costa, and T. Surrey. 2020. Microtubule Nucleation Properties of Single Human γTuRCs Explained by Their Cryo-EM Structure. *Dev Cell*. doi:10.1016/j.devcel.2020.04.019.

Cota, R.R., N. Teixidó-Travesa, A. Ezquerra, S. Eibes, C. Lacasa, J. Roig, and J. Lüders. 2017. MZT1 regulates microtubule nucleation by linking γTuRC assembly to adapter-mediated targeting and activation. *J Cell Sci*. 130:jcs.195321. doi:10.1242/jcs.195321.

Cullen, C.F., P. Deák, D.M. Glover, and H. Ohkura. 1999. mini spindles: A gene encoding a conserved microtubule-associated protein required for the integrity of the mitotic spindle in Drosophila. *The Journal of cell biology*. 146:1005 1018.

Dobbelaere, J., F. Josué, S. Suijkerbuijk, B. Baum, N. Tapon, and J. Raff. 2008. A genome-wide RNAi screen to dissect centriole duplication and centrosome maturation in Drosophila. *Plos Biol*. 6:e224. doi:10.1371/journal.pbio.0060224.

Farache, D., L. Emorine, L. Haren, and A. Merdes. 2018. Assembly and regulation of γ-tubulin complexes. *Open Biol*. 8:170266. doi:10.1098/rsob.170266.

Flor-Parra, I., A.B. Iglesias-Romero, and F. Chang. 2018. The XMAP215 Ortholog Alp14 Promotes Microtubule Nucleation in Fission Yeast. *Curr Biol*. 28:1681 1691.e4. doi:10.1016/j.cub.2018.04.008.

Fong, K.-W., Y.-K. Choi, J.B. Rattner, and R.Z. Qi. 2008. CDK5RAP2 is a pericentriolar protein that functions in centrosomal attachment of the gamma-tubulin ring complex. *Mol Biol Cell*. 19:115 125. doi:10.1091/mbc.e07-04-0371.

Gao, X., M. Schmid, Y. Zhang, S. Fukuda, N. Takeshita, and R. Fischer. 2019. The spindle pole body of Aspergillus nidulans is asymmetrically composed with changing numbers of gamma-tubulin complexes. *J Cell Sci*. 132:jcs.234799. doi:10.1242/jcs.234799.

Ghosh, S., C. Hentrich, and T. Surrey. 2013. Micropattern-Controlled Local Microtubule Nucleation, Transport, and Mesoscale Organization. *Acs Chem Biol*. 8:673–678. doi:10.1021/cb300583p.

Gomez-Ferreria, M.A., M. Bashkurov, A.O. Helbig, B. Larsen, T. Pawson, A.-C. Gingras, and L. Pelletier. 2012a. Novel NEDD1 phosphorylation sites regulate γ-tubulin binding and mitotic spindle assembly. *J Cell Sci*. 125:3745 3751. doi:10.1242/jcs.105130.

Gomez-Ferreria, M.A., M. Bashkurov, M. Mullin, A.-C. Gingras, and L. Pelletier. 2012b. CEP192 interacts physically and functionally with the K63-deubiquitinase CYLD to promote mitotic spindle assembly. *Cell Cycle*. 11:3555–3558. doi:10.4161/cc.21574.

Gomez-Ferreria, M.A., U. Rath, D.W. Buster, S.K. Chanda, J.S. Caldwell, D.R. Rines, and D.J. Sharp. 2007. Human Cep192 is required for mitotic centrosome and spindle assembly. *Curr Biol*. 17:1960 1966. doi:10.1016/j.cub.2007.10.019.

Goshima, G. 2011. Identification of a TPX2-like microtubule-associated protein in Drosophila. *Plos One*. 6:e28120. doi:10.1371/journal.pone.0028120.

Groen, A.C., T.J. Maresca, J.C. Gatlin, E.D. Salmon, and T.J. Mitchison. 2009. Functional Overlap of Microtubule Assembly Factors in Chromatin-Promoted Spindle Assembly. *Mol Biol Cell*. 20:2766–2773. doi:10.1091/mbc.e09-01-0043.

Gunzelmann, J., D. Rüthnick, T. Lin, W. Zhang, A. Neuner, U. Jäkle, and E. Schiebel. 2018a. The microtubule polymerase Stu2 promotes oligomerization of the γ-TuSC for cytoplasmic microtubule nucleation. *Elife*. 7:e39932. doi:10.7554/elife.39932.

Gunzelmann, J., D. Rüthnick, T. Lin, W. Zhang, A. Neuner, U. Jäkle, and E. Schiebel. 2018b. The microtubule polymerase Stu2 promotes oligomerization of the γ-TuSC for cytoplasmic microtubule nucleation. *Elife*. 7:934. doi:10.7554/elife.39932.

Hannak, E., K. Oegema, M. Kirkham, P. Gönczy, B. Habermann, and A.A. Hyman. 2002. The kinetically dominant assembly pathway for centrosomal asters in Caenorhabditis elegans is γ-tubulin dependent. *J Cell Biology*. 157:591–602. doi:10.1083/jcb.200202047.

Haren, L., D. Farache, L. Emorine, and A. Merdes. 2020. A stable sub-complex between GCP4, GCP5 and GCP6 promotes the assembly of γ-tubulin ring complexes. *J Cell Sci*. jcs.244368. doi:10.1242/jcs.244368.

Haren, L., M.-H. Remy, I. Bazin, I. Callebaut, M. Wright, and A. Merdes. 2006. NEDD1-dependent recruitment of the γ-tubulin ring complex to the centrosome is necessary for centriole duplication and spindle assembly. *J Cell Biology*. 172:505–515. doi:10.1083/jcb.200510028.

Haren, L., T. Stearns, and J. Lüders. 2009. Plk1-dependent recruitment of gamma-tubulin complexes to mitotic centrosomes involves multiple PCM components. *Plos One*. 4:e5976. doi:10.1371/journal.pone.0005976.

Huang, T.-L., H.-J. Wang, Y.-C. Chang, S.-W. Wang, and K.-C. Hsia. 2020. Promiscuous Binding of Microprotein Mozart1 to γ-Tubulin Complex Mediates Specific Subcellular Targeting to Control Microtubule Array Formation. *Cell Reports*. 31:107836. doi:10.1016/j.celrep.2020.107836.

Imasaki, T., S. Kikkawa, S. Niwa, Y. Saijo-Hamano, H. Shigematsu, K. Aoyama, K. Mitsuoka, T. Shimizu, M. Aoki, A. Sakamoto, Y. Tomabechi, N. Sakai, M. Shirouzu, S. Taguchi, Y. Yamagishi, T. Setsu, Y. Sakihama, E. Nitta, M. Takeichi, and R. Nitta. 2022. CAMSAP2 organizes a γ-tubulin-independent microtubule nucleation centre through phase separation. *Elife*. 11:e77365. doi:10.7554/elife.77365.

Khodjakov, A., and C.L. Rieder. 1999. The sudden recruitment of gamma-tubulin to the centrosome at the onset of mitosis and its dynamic exchange throughout the cell cycle, do not require microtubules. *The Journal of cell biology*. 146:585 596.

King, B.R., M. Moritz, H. Kim, D.A. Agard, C.L. Asbury, and T.N. Davis. 2020. XMAP215 and γ-tubulin additively promote microtubule nucleation in purified solutions. *Mol Biol Cell*. mbcE20020160. doi:10.1091/mbc.e20-02-0160.

Kitamura, E., K. Tanaka, S. Komoto, Y. Kitamura, C. Antony, and T.U. Tanaka. 2010. Kinetochores Generate Microtubules with Distal Plus Ends: Their Roles and Limited Lifetime in Mitosis. *Dev Cell*. 18:248–259. doi:10.1016/j.devcel.2009.12.018.

Kollman, J.M., A. Merdes, L. Mourey, and D.A. Agard. 2011. Microtubule nucleation by γ-tubulin complexes. *Nat Rev Mol Cell Bio*. 12:709 721. doi:10.1038/nrm3209.

Kollman, J.M., J.K. Polka, A. Zelter, T.N. Davis, and D.A. Agard. 2010. Microtubule nucleating gamma-TuSC assembles structures with 13-fold microtubule-like symmetry. *Nature*. 466:879 882. doi:10.1038/nature09207.

Lee, K., and K. Rhee. 2011. PLK1 phosphorylation of pericentrin initiates centrosome maturation at the onset of mitosis. *J Cell Biology*. 195:1093–1101. doi:10.1083/jcb.201106093.

Lee, M.J., F. Gergely, K. Jeffers, S.Y. Peak-Chew, and J.W. Raff. 2001. Msps/XMAP215 interacts with the centrosomal protein D-TACC to regulate microtubule behaviour. *Nat Cell Biol*. 3:643 649. doi:10.1038/35083033.

Lin, T., A. Neuner, Y.T. Schlosser, E. Schiebel, A.N. Scharf, and L. Weber. 2014. Cell-cycle dependent phosphorylation of yeast pericentrin regulates γ-TuSC-mediated microtubule nucleation. *Elife*. 3:e02208. doi:10.7554/elife.02208.

Lucas, E.P., and J.W. Raff. 2007. Maintaining the proper connection between the centrioles and the pericentriolar matrix requires Drosophila Centrosomin. *J Cell Biology*. 178:725–732. doi:10.1083/jcb.200704081.

Lüders, J., U.K. Patel, and T. Stearns. 2006. GCP-WD is a gamma-tubulin targeting factor required for centrosomal and chromatin-mediated microtubule nucleation. *Nat Cell Biol*. 8:137 147. doi:10.1038/ncb1349.

Lyon, A.S., G. Morin, M. Moritz, K.C.B. Yabut, T. Vojnar, A. Zelter, E. Muller, T.N. Davis, and D.A. Agard. 2016. Higher-order oligomerization of Spc110p drives γ-tubulin ring complex assembly. *Mol Biol Cell*. 27:mbc.E16-02-0072 2258. doi:10.1091/mbc.e16-02-0072.

Martinez-Campos, M., R. Basto, J. Baker, M. Kernan, and J.W. Raff. 2004. The Drosophila pericentrin-like protein is essential for cilia/flagella function, but appears to be dispensable for mitosis. *J Cell Biology*. 165:673–683. doi:10.1083/jcb.200402130.

Mukherjee, A., P.S. Brooks, F. Bernard, A. Guichet, and P.T. Conduit. 2020. Microtubules originate asymmetrically at the somatic Golgi and are guided via Kinesin2 to maintain polarity in neurons. *Elife*. 9:e58943. doi:10.7554/elife.58943.

Muroyama, A., L. Seldin, and T. Lechler. 2016. Divergent regulation of functionally distinct γ-tubulin complexes during differentiation. *J Cell Biology*. 213:679–692. doi:10.1083/jcb.201601099.

Nakaoka, Y., A. Kimura, T. Tani, and G. Goshima. 2015. Cytoplasmic nucleation and atypical branching nucleation generate endoplasmic microtubules in Physcomitrella patens. *Plant Cell Online*. 27:228 242. doi:10.1105/tpc.114.134817.

Nashchekin, D., A.R. Fernandes, and D.S. Johnston. 2016. Patronin/Shot Cortical Foci Assemble the Noncentrosomal Microtubule Array that Specifies the Drosophila Anterior-Posterior Axis. *Dev Cell*. 38:61 72. doi:10.1016/j.devcel.2016.06.010.

Oakley, B.R., V. Paolillo, and Y. Zheng. 2015. γ-Tubulin complexes in microtubule nucleation and beyond. *Mol Biol Cell*. 26:2957–2962. doi:10.1091/mbc.e14-11-1514.

Piehl, M., U.S. Tulu, P. Wadsworth, and L. Cassimeris. 2004. Centrosome maturation: measurement of microtubule nucleation throughout the cell cycle by using GFP-tagged EB1. *P Natl Acad Sci Usa*. 101:1584 1588. doi:10.1073/pnas.0308205100.

Popov, A.V., F. Severin, and E. Karsenti. 2002. XMAP215 Is Required for the Microtubule-Nucleating Activity of Centrosomes. *Curr Biol*. 12:1326–1330. doi:10.1016/s0960-9822(02)01033-3.

Popova, J.V., G.A. Pavlova, A.V. Razuvaeva, L.A. Yarinich, E.N. Andreyeva, A.F. Anders, Y.A. Galimova, F. Renda, M.P. Somma, A.V. Pindyurin, and M. Gatti. 2022. Genetic Control of Kinetochore-Driven Microtubule Growth in Drosophila Mitosis. *Cells*. 11:2127. doi:10.3390/cells11142127.

Port, F., H.-M. Chen, T. Lee, and S.L. Bullock. 2014. Optimized CRISPR/Cas tools for efficient germline and somatic genome engineering in Drosophila. *Proc National Acad Sci*. 111:E2967–E2976. doi:10.1073/pnas.1405500111.

Reschen, R.F., N. Colombié, L. Wheatley, J. Dobbelaere, D.S. Johnston, H. Ohkura, and J.W. Raff. 2012. Dgp71WD is required for the assembly of the acentrosomal Meiosis I spindle, and is not a general targeting factor for the γ-TuRC. *Biol Open*. 1:422 429. doi:10.1242/bio.2012596.

Rogers, G.C., N.M. Rusan, M. Peifer, and S.L. Rogers. 2008. A multicomponent assembly pathway contributes to the formation of acentrosomal microtubule arrays in interphase Drosophila cells. *Mol Biol Cell*. 19:3163 3178. doi:10.1091/mbc.e07-10-1069.

Roostalu, J., N.I. Cade, and T. Surrey. 2015. Complementary activities of TPX2 and chTOG constitute an efficient importin-regulated microtubule?nucleation module. *Nat Cell Biol*. 17:1422 1434. doi:10.1038/ncb3241.

Sallee, M.D., J.C. Zonka, T.D. Skokan, B.C. Raftrey, and J.L. Feldman. 2018. Tissue-specific degradation of essential centrosome components reveals distinct microtubule populations at microtubule organizing centers. *Plos Biol*. 16:e2005189. doi:10.1371/journal.pbio.2005189.

Samejima, I., V.J. Miller, L.M. Groocock, and K.E. Sawin. 2008. Two distinct regions of Mto1 are required for normal microtubule nucleation and efficient association with the gamma-tubulin complex in vivo. *J Cell Sci*. 121:3971 3980. doi:10.1242/jcs.038414.

Sampaio, P., E. Rebollo, H. Varmark, C.E. Sunkel, and C. González. 2001. Organized microtubule arrays in γ-tubulin-depleted Drosophila spermatocytes. *Current biology : CB*. 11:1788 1793. doi:10.1016/s0960-9822(01)00561-9.

Sawin, K.E., P.C.C. Lourenço, and H.A. Snaith. 2004. Microtubule nucleation at non-spindle pole body microtubule-organizing centers requires fission yeast centrosomin-related protein mod20p. *Curr Biol*. 14:763 775. doi:10.1016/j.cub.2004.03.042.

Schatz, C.A., R. Santarella, A. Hoenger, E. Karsenti, I.W. Mattaj, O.J. Gruss, and R.E. Carazo-Salas. 2003. Importin α-regulated nucleation of microtubules by TPX2. *Embo J*. 22:2060–2070. doi:10.1093/emboj/cdg195.

Slep, K.C., and R.D. Vale. 2007. Structural Basis of Microtubule Plus End Tracking by XMAP215, CLIP-170, and EB1. *Mol Cell*. 27:976–991. doi:10.1016/j.molcel.2007.07.023.

Strome, S., J. Powers, M. Dunn, K. Reese, C.J. Malone, J. White, G. Seydoux, and W. Saxton. 2001. Spindle Dynamics and the Role of γ-Tubulin in

EarlyCaenorhabditis elegans Embryos. *Mol Biol Cell*. 12:1751–1764. doi:10.1091/mbc.12.6.1751.

Sunkel, C.E., R. Gomes, P. Sampaio, J. Perdigão, and C. González. 1995. Gamma-tubulin is required for the structure and function of the microtubule organizing centre in Drosophila neuroblasts. *Embo J*. 14:28–36. doi:10.1002/j.1460-2075.1995.tb06972.x.

Thawani, A., R.S. Kadzik, and S. Petry. 2018. XMAP215 is a microtubule nucleation factor that functions synergistically with the γ-tubulin ring complex. *Nat Cell Biol*. 20:1 18. doi:10.1038/s41556-018-0091-6.

Tovey, C.A., and P.T. Conduit. 2018. Microtubule nucleation by γ-tubulin complexes and beyond. *Essays Biochem*. 91:EBC20180028. doi:10.1042/ebc20180028.

Tovey, C.A., C. Tsuji, A. Egerton, F. Bernard, A. Guichet, M. de la Roche, and P.T. Conduit. 2021. Autoinhibition of Cnn binding to γ-TuRCs prevents ectopic microtubule nucleation and cell division defects. *J Cell Biol*. 220:e202010020. doi:10.1083/jcb.202010020.

Tovey, C.A., C.E. Tubman, E. Hamrud, Z. Zhu, A.E. Dyas, A.N. Butterfield, A. Fyfe, E. Johnson, and P.T. Conduit. 2018. γ-TuRC Heterogeneity Revealed by Analysis of Mozart1. *Curr Biol*. 28:2314 2323.e6. doi:10.1016/j.cub.2018.05.044.

Tsuchiya, K., and G. Goshima. 2021. Microtubule-associated proteins promote microtubule generation in the absence of γ-tubulin in human colon cancer cells. *J Cell Biol*. 220:e202104114. doi:10.1083/jcb.202104114.

Vérollet, C., N. Colombié, T. Daubon, H.-M. Bourbon, M. Wright, and B. Raynaud-Messina. 2006. Drosophila melanogaster γ-TuRC is dispensable for targeting γ-tubulin to the centrosome and microtubule nucleation. *J Cell Biology*. 172:517–528. doi:10.1083/jcb.200511071.

Vogt, N., I. Koch, H. Schwarz, F. Schnorrer, and C. Nüsslein-Volhard. 2006. The γTuRC components Grip75 and Grip128 have an essential microtubule-anchoring function in the Drosophila germline. *Development*. 133:3963–3972. doi:10.1242/dev.02570.

Wang, S., D. Wu, S. Quintin, R.A. Green, D.K. Cheerambathur, S.D. Ochoa, A. Desai, and K. Oegema. 2015. NOCA-1 functions with γ-tubulin and in parallel to Patronin to assemble non-centrosomal microtubule arrays in C. elegans. *Elife*. 4:e08649. doi:10.7554/elife.08649.

Wieczorek, M., S. Bechstedt, S. Chaaban, and G.J. Brouhard. 2015. Microtubule-associated proteins control the kinetics of microtubule nucleation. *Nat Cell Biol*. 17:907 916. doi:10.1038/ncb3188.

Wieczorek, M., T.-L. Huang, L. Urnavicius, K.-C. Hsia, and T.M. Kapoor. 2020. MZT Proteins Form Multi-Faceted Structural Modules in the γ-Tubulin Ring Complex. *Cell Reports*. 31:107791. doi:10.1016/j.celrep.2020.107791.

Wieczorek, M., L. Urnavicius, S.-C. Ti, K.R. Molloy, B.T. Chait, and T.M. Kapoor. 2019. Asymmetric Molecular Architecture of the Human γ-Tubulin Ring Complex. *Cell*. doi:10.1016/j.cell.2019.12.007.

Woodruff, J.B., B.F. Gomes, P.O. Widlund, J. Mahamid, A. Honigmann, and A.A. Hyman. 2017. The Centrosome Is a Selective Condensate that Nucleates Microtubules by Concentrating Tubulin. *Cell*. 169:1066 1077.e10. doi:10.1016/j.cell.2017.05.028.

Würtz, M., E. Zupa, E.S. Atorino, A. Neuner, A. Böhler, A.S. Rahadian, B.J.A. Vermeulen, G. Tonon, S. Eustermann, E. Schiebel, and S. Pfeffer. 2022. Modular assembly of the principal microtubule nucleator γ-TuRC. *Nat Commun*. 13:473. doi:10.1038/s41467-022-28079-0.

Xiong, Y., and B.R. Oakley. 2009. In vivo analysis of the functions of gamma-tubulin-complex proteins. *J Cell Sci*. 122:4218 4227. doi:10.1242/jcs.059196.

Yang, S.Z., and J. Wildonger. 2020. Golgi Outposts Locally Regulate Microtubule Orientation in Neurons but Are Not Required for the Overall Polarity of the Dendritic Cytoskeleton. *Genetics*. 215:435–447. doi:10.1534/genetics.119.302979.

Zhang, J., and T.L. Megraw. 2007. Proper recruitment of gamma-tubulin and D-TACC/Msps to embryonic Drosophila centrosomes requires Centrosomin Motif 1. *Mol Biol Cell*. 18:4037 4049. doi:10.1091/mbc.e07-05-0474.

Zhang, L., T.J. Keating, A. Wilde, G.G. Borisy, and Y. Zheng. 2000. The role of Xgrip210 in gamma-tubulin ring complex assembly and centrosome recruitment. *The Journal of cell biology*. 151:1525 1536.

Zhang, X., Q. Chen, J. Feng, J. Hou, F. Yang, J. Liu, Q. Jiang, and C. Zhang. 2009. Sequential phosphorylation of Nedd1 by Cdk1 and Plk1 is required for targeting of the γTuRC to the centrosome. *J Cell Sci*. 122:2240–2251. doi:10.1242/jcs.042747.

Zheng, Y., R.A. Buchwalter, C. Zheng, E.M. Wight, J.V. Chen, and T.L. Megraw. 2020. A perinuclear microtubule-organizing centre controls nuclear positioning and basement membrane secretion. *Nat Cell Biol*. 22:297–309. doi:10.1038/s41556-020-0470-7.

Zimmerman, W.C., J. Sillibourne, J. Rosa, and S.J. Doxsey. 2004. Mitosis-specific anchoring of gamma tubulin complexes by pericentrin controls spindle organization and mitotic entry. *Mol Biol Cell*. 15:3642 3657. doi:10.1091/mbc.e03-11-0796.

Figure Legends

Figure 1

Cnn recruits γ-tubulin complexes via its CM1 domain and independently of Grip71 and the GCP4/5/4/6 core. (A) Fluorescence images of either interphase or mitotic *Drosophila* brain cells from either wild-type, *spd-2* mutant, or *spd-2, grip71,grip75*^{GCP4}*,grip128*^{GCP5}-RNAi,*grip163*^{GCP6} mutant third instar larval brains immunostained for γ-tubulin (green), mitotic DNA (blue), and Asl (centrioles, magenta). Both mutants carry the mutant *spd-2* alleles, to reveal the Cnn pathway of recruitment. Error bar is 5μm and applies to all images. **(B)** Graph showing average fluorescence intensities (relative to wild-type) of interphase (blue dots) and mitotic (black dots) centrosomes from different genotypes (as indicated below). Each data-point represents the average centrosome value from one brain. Mean and SEM are indicated. Paired t-tests were used to compare mean values of interphase and mitotic centrosomes within each genotype. Note the similarity in mitotic centrosomal γ-tubulin levels in *spd-2* mutants and in *spd-2, grip71,grip75*^{GCP4}*, grip128*^{GCP5}-RNAi,*grip163*^{GCP6} mutants, showing that Cnn can recruit γ-tubulin complexes to mitotic centrosomes when only γ-TuSCs are present. **(C)** Fluorescence images of either interphase or mitotic *Drosophila* brain cells from either wild-type or *cnn*$^{\Delta CM1}$,*spd-2* mutant third instar larval brains immunostained for γ-tubulin (green), mitotic DNA (blue), and Asl (centrioles, magenta). Scale bar is 5μm and applies to all images. **(D)** Graph in the same format as in (B) revealing no significant increase of centrosomal γ-tubulin signal from interphase to mitosis in *cnn*$^{\Delta CM1}$;*spd-2* mutant cells, showing that Cnn requires its CM1 domain to recruit γ-tubulin complexes to centrosomes. **(E)** Multi-protein sequence alignment of part of the CM1 domain containing the key binding residues (indicated by red boxes) in budding yeast and humans that we mutated in *Drosophila*. **(F)** Western blot probed for MBP and γ-tubulin showing the results of IP experiments from embryo extracts using bacterially purified MBP-tagged N-terminal (aa1-255) Cnn fragments containing point mutations to relieve Cnn-C autoinhibition (T27E and S186D; Tovey et al., 2021) and to perturb the CM1 domain's ability to bind γ-TuRCs (R101Q, E102A, and F115A).

Figure 2

Recruitment of γ-tubulin complexes by Spd-2 is heavily dependent on the GCP4/5/4/6 core (A) Fluorescence images of mitotic *Drosophila* brain cells from wild-type or mutant third instar larvae immunostained for γ-tubulin (green), mitotic DNA (blue), and Asl (centrioles, magenta). All mutants carry the mutant *cnn* alleles, to reveal the Spd-2 pathway of recruitment, along with mutant alleles for different combinations of γ-TuRC genes. Scale bar is 5μm and applies to all images. **(B)** Graph showing average fluorescence intensities (relative to wild-type) of interphase (blue dots) and mitotic (black dots) centrosomes from different genotypes (as indicated below). Each data-point represents the average centrosome value from one brain. Mean and SEM are indicated. Paired t-tests were used to compare mean values of interphase and mitotic centrosomes within each genotype. Note that γ-tubulin accumulation at mitotic centrosomes is severely perturbed in the absence of the GCP4/5/4/6 core components Grip75^{GCP4} and Grip163^{GCP6}, but is abolished only in the absence of Grip71 and Grip163^{GCP6}. **(C)** Fluorescence images of mitotic *Drosophila* brain cells from wild-type or *cnn,grip71,grip163* mutant third instar larvae immunostained for Spd-2 (green), mitotic DNA (blue), and Asl (centrioles, magenta). Scale bar is 5μm and applies to both images. **(D)** Graph in the same format as in (B) showing a significant increase of centrosomal Spd-2 signal from interphase to mitosis in *cnn,grip71,grip163* mutant cells, showing that the inability of these centrosomes to recruit γ-tubulin (A,B) is not due to an absence of Spd-2. **(E)** Diagram summarising how Cnn can recruit γ-TuSCs while Spd-2 recruitment relies largely on pre-formed γ-TuRCs.

Figure 3

Mitotic centrosomes lacking γ-tubulin can still nucleate microtubules. (A-C) Fluorescence images of mitotic *Drosophila* brain cells from either wild-type or *cnn,grip71,grip163* mutant third instar larval brains, either at steady state (A), after 40 minutes of cooling on ice (B), or after 30s of warming (post cooling) to room temperature (C) immunostained for alpha-tubulin (microtubules, green), mitotic DNA (blue), and Asl (centrioles, magenta). Note how centrosomes in both wild-type and

cnn,grip71,grip163 mutant cells are associated with microtubules both at steady state and after 30s warming. (**D-F**) Fluorescent images (D,E) and graph (F) documenting the behaviour of the microtubule marker Jupiter-mCherry within living *Drosophila* control (D) or *cnn,grip71,grip163* mutant (E) third instar larval brain cells as they were cooled to 5˚C for ~3 minutes and then rapidly warmed to 20˚C. Time in seconds relative to the initiation of warming (0s) is indicated. Note that the GFP-PACT signal used to locate centrosomes is not displayed. The graph in (F) plots the mean and SEM centrosomal signal (after subtraction of cytosolic signal) of 12 and 10 centrosomes from control and *cnn,grip71,grip163* mutant cells, respectively. The data is normalised to the average signal at centrosomes in control cells prior to cooling. Note how the centrosomal Jupiter-mCherry signal quickly drops on cooling and then immediately increases on warming in both control and *cnn,grip71,grip163* mutant cells, showing that centrosomes within both control and *cnn,grip71,grip163* mutant cells nucleate microtubules. (**G,H**) Graphs show the depolymerisation (G) and nucleation/regrowth phases (H) phases from the graph in (F). One-phase exponential decay models and "exponential plateau" models are fitted to the depolymerisation and nucleation/regrowth phases, respectively. Note how the centrosomal Jupiter-mCherry signal decreases faster upon cooling, but increases slower upon warming, in *cnn,grip71,grip163* mutant cells. (**I,J**) Fluorescent images documenting the behaviour of the microtubule plus-end marker EB1-GFP within living *Drosophila* control (I) and *cnn,grip71,grip163* mutant (J) third instar larval brain cells as they were cooled to 5˚C and then rapidly warmed to 20˚C. Time in seconds relative to the initiation of warming (0s) is indicated. Note how the EB1-GFP signal emanates from the centrosome and from the spindle/chromatin region during warming in the *cnn,grip71,grip163* mutant cell.

Figure 4

Depletion of Msps strongly perturbs the ability of centrosomes to organise microtubules in the absence of γ-tubulin complexes. (A-E) Fluorescence images of *Drosophila* brain cells in either prophase or prometaphase from either wild-type (A), *cnn,grip71,grip163* (B), *cnn,grip71,grip163,msps* (C), *cnn,grip71,grip163,tacc* (D), or *cnn,grip71,grip163,mei38-RNAi* cell (E) immunostained for alpha-tubulin

(microtubules, green), mitotic DNA (blue), and Asl (centrioles, magenta). **(F)** Graph showing the percentage of prophase cells in which microtubules are associated with at least one centrosome within the various genotypes, as indicated. The number of cells analysed (n) is indicated. Datasets were compared to the *cnn,grip71,grip163* dataset using one-way Chi-squared tests. Note how there is a no significant reduction between wild-type and *cnn,grip71,grip163* mutant cells in the proportion of cells displaying centrosome-associated microtubules, but there are significant reductions between *cnn,grip71,grip163* mutant cells and cells that are also depleted for either Msps, TACC or *mei*-38, indicating that Msps, TACC and *mei*-38 have a role in γ-TuRC-independent microtubule nucleation. **(G, H)** Graphs of raw data (G) and log transformed data (H) showing the distance of centrosomes from spindle poles during prometaphase in the different genotypes, as indicated. The percentage of centrosomes that were further than 1μm from the spindle poles is indicated above each dataset in the graph in (G). Increased distance from the spindle pole is indicative of a failure to properly organise microtubules. Kruskal-Wallis tests were used to compare the distribution of the *cnn,grip71,grip163* dataset with those of the other genotypes. Note that there is a significant difference only between *cnn,grip71,grip163* and *cnn,grip71,grip163,msps* mutant cells, indicating that Msps is particularly important for microtubule organisation at centrosomes in the absence of γ-TuRCs.

Figure 5

Msps plays an important role in γ-TuRC-independent microtubule nucleation from centrosomes. (A-E) Parts of a whole graphs (A,C,E) and images (B,D) represent analyses of either centrosomal aster types (A,B) or mitotic spindle quality (C-E) in cells fixed and immunostained for alpha-tubulin (microtubules, green), mitotic DNA (blue), and Asl (centrioles, magenta) after 30 seconds of warming post cooling from either *cnn,grip71,grip163* or *cnn,grip71,grip163,msps* mutants, as indicated. Only cells that had centrosomes but that had not yet formed a spindle were analysed in A,B; only cells that had centrosomes and that had already formed a spindle were analysed in (C,D); and only cells lacking centrosomes but that had formed a spindle were analysed in (E). Note how centrosome asters are frequently absent in *cnn,grip71,grip163,msps* (A,B) and that spindle quality is frequently low (C,D), but the

difference in spindle quality between mutant types is not apparent in cells lacking centrosomes (E).

Figure S1

***Drosophila* centrosomes do not concentrate a/β-tubulin.** Fluorescence images of mitotic *Drosophila* brain cells from wild-type third instar larval brains that had been cooled for 40 minutes on ice immunostained for alpha-tubulin (microtubules, green), mitotic DNA (blue), and Asl (centrioles, magenta). Note how there is no tubulin signal at centrosomes that is above cytosolic levels.

Figure S2

***Drosophila* centrosomes do not concentrate a/β-tubulin. (A,B)** Graphs plotting the centrosomal signal (after subtraction of cytosolic signal) of Jupiter-mCherry within living *Drosophila* control (D) and *cnn,grip71,grip163* mutant (E) third instar larval brain cells as they were cooled to 5˚C for ~3 minutes and then rapidly warmed to 20˚C. Time in seconds relative to the initiation of warming (0s) is indicated. Note how the centrosomal Jupiter-mCherry signal does not always reach cytosolic levels (i.e. 0), indicating that microtubules were not fully depolymerised from all centrosomes, but note also that even when the Jupiter-mCherry signal did reach cytosolic levels there was still a rapid increase after warming, indicating that the increase in signal after warming is not simply due to regrowth of partially depolymerised microtubules.

Figure S3

The distribution of cells with and without centrosomes and with and without re-formed spindles is similar in *cnn,grip71,grip163* mutant and *cnn,grip71,grip163,msps* mutant cells after 30 seconds of warming post cooling. Parts of a whole graphs show the proportion of cells that either contain centrosomes or do not, and that have either formed a spindle or have not, in cells fixed and immunostained for alpha-tubulin (microtubules, green), mitotic DNA (blue), and Asl (centrioles, magenta) after 30 seconds of warming post cooling from either *cnn,grip71,grip163* or *cnn,grip71,grip163,msps* mutants, as indicated.

Supplementary Videos

Video 1

Microtubule depolymerisation and regrowth at centrosomes in control cells. Video showing the Jupiter-mCherry signal (marking microtubules) within a living control cell during a cooling-warming experiment. Cooling to 5˚C begins at -174s and warming to 20˚C begins at 0s. Note how the Jupiter-mCherry signal decreases gradually during cooling and then recovers immediately at the two centrosomes during warming.

Video 2

Microtubule depolymerisation and regrowth at centrosomes in *cnn,grip71,grip163* mutant cells. Video showing the Jupiter-mCherry signal (marking microtubules) within a living *cnn,grip71,grip163 mutant* cell during a cooling-warming experiment. Cooling to 5˚C begins at -186s and warming to 20˚C begins at 0s. Only one centrosome is present (spindle pole on the left). Note how the Jupiter-mCherry signal decreases gradually during cooling and then recovers immediately at the centrosome during warming, but that this recovery is slower and less intense than in control cells.

Video 3

Behaviour of EB1-GFP comets at centrosomes during a cooling-warming cycle in control cells. Video showing the EB1-GFP signal (marking growing microtubule ends) within a living control cell during a cooling-warming experiment. Cooling to 5˚C begins at -54s and warming to 20˚C begins at 0s. Note how the EB1-GFP signal disappears immediately on cooling and then dramatically reappears and spreads outwards from the two centrosomes during warming.

Video 4

Behaviour of EB1-GFP comets at centrosomes during a cooling-warming cycle in *cnn,grip71,grip163 mutant* cells. Video showing the EB1-GFP signal (marking growing microtubule ends) within a **living *cnn,grip71,grip163* mutant** cell during a

cooling-warming experiment. Cooling to 5˚C begins at -276s and warming to 20˚C begins at 0s. Note how the EB1-GFP signal does not disappear immediately on cooling, unlike in control cells. The signal does disappear fully prior to warming and then reappears from the centrosomes and chromosomal regions during warming, spreading outwards. Note also that the centrosomes do not remain in focus throughout the movie. The centrosome at the spindle pole in the lower half of the cell is in focus throughout most of the movie, but this centrosome is out of focus for ~30s after warming due to fluctuations in the cover glass during the temperature change.

Figure 1

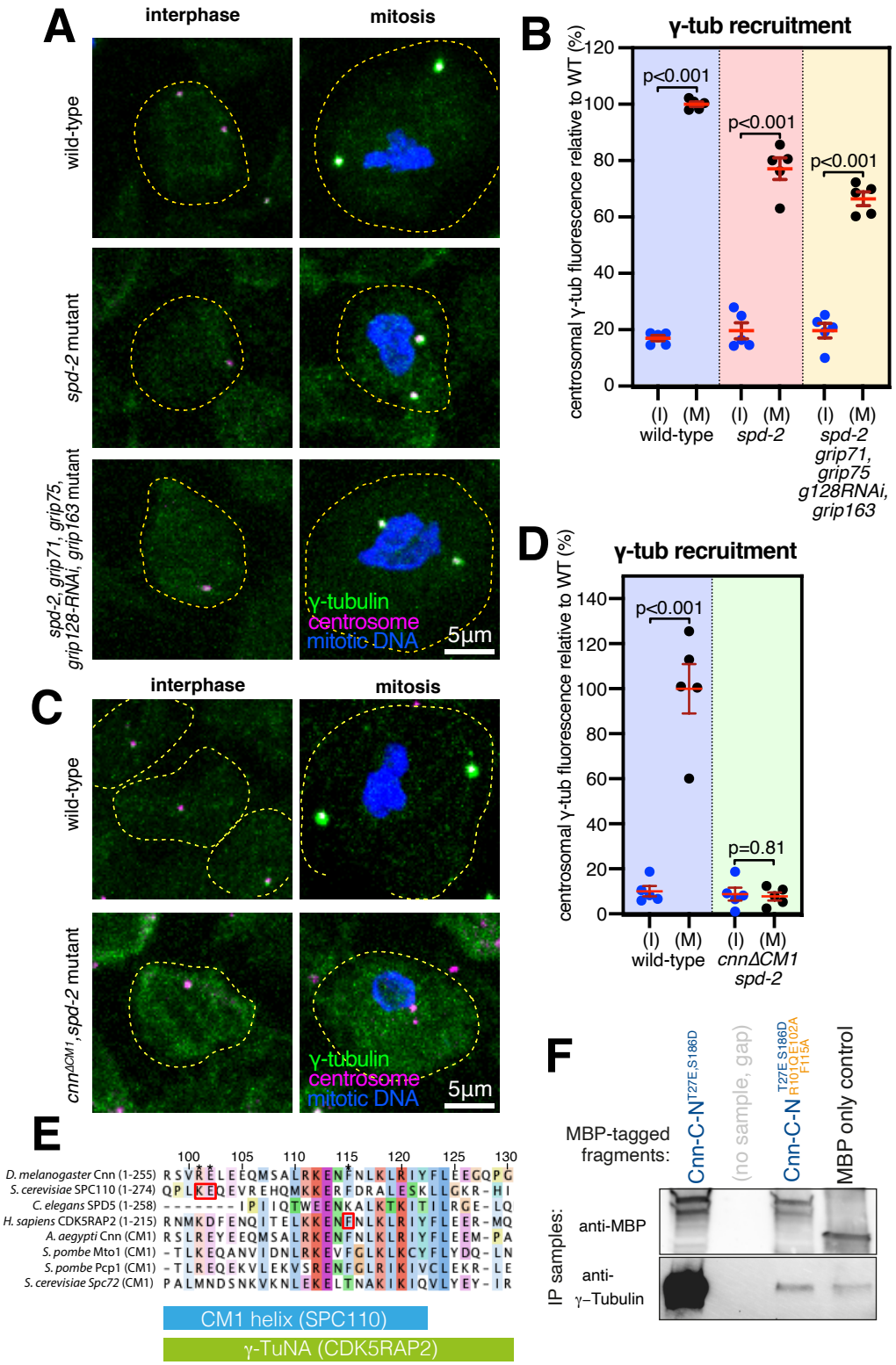
A
interphase
mitosis
wild-type
spd-2 mutant
spd-2, grip71, grip75, grip128-RNAi, grip163 mutant
γ-tubulin
centrosome
mitotic DNA
5µm
B
γ-tub recruitment
centrosomal γ-tub fluorescence relative to WT (%)
p<0.001
p<0.001
p<0.001
(I) (M) wild-type
(I) (M) spd-2
(I) (M) spd-2 grip71, grip75 g128RNAi, grip163
C
interphase
mitosis
wild-type
cnnΔCM1,spd-2 mutant
γ-tubulin
centrosome
mitotic DNA
5µm
D
γ-tub recruitment
centrosomal γ-tub fluorescence relative to WT (%)
p<0.001
p=0.81
(I) (M) wild-type
(I) (M) cnnΔCM1 spd-2
E
D. melanogaster Cnn (1-255)
S. cerevisiae SPC110 (1-274)
C. elegans SPD5 (1-258)
H. sapiens CDK5RAP2 (1-215)
A. aegypti Cnn (CM1)
S. pombe Mto1 (CM1)
S. pombe Pcp1 (CM1)
S. cerevisiae Spc72 (CM1)
CM1 helix (SPC110)
γ-TuNA (CDK5RAP2)
F
MBP-tagged fragments:
Cnn-C-N T27E,S186D
(no sample, gap)
Cnn-C-N T27E S186D R101QE102A F115A
MBP only control
IP samples:
anti-MBP
anti-γ-Tubulin

Figure 2

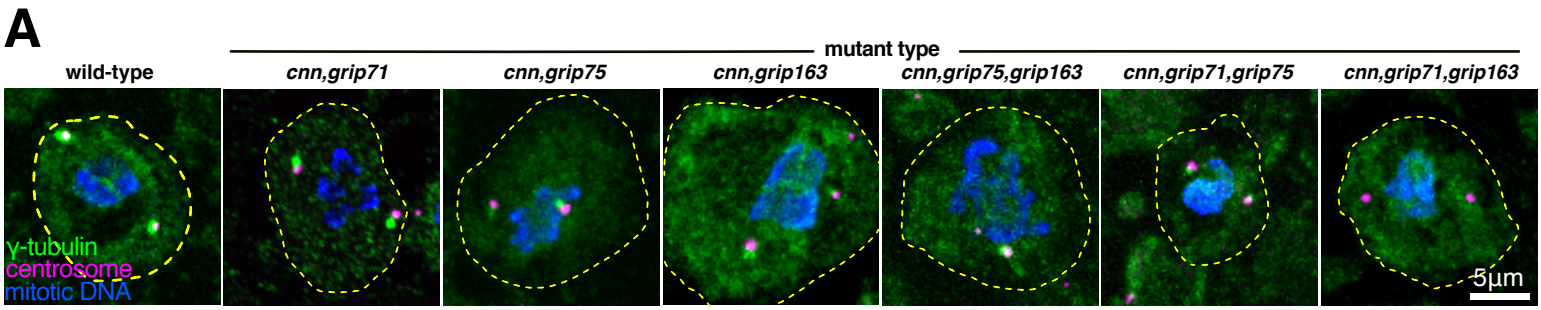
A
mutant type
wild-type
cnn,grip71
cnn,grip75
cnn,grip163
cnn,grip75,grip163
cnn,grip71,grip75
cnn,grip71,grip163
γ-tubulin
centrosome
mitotic DNA
5µm

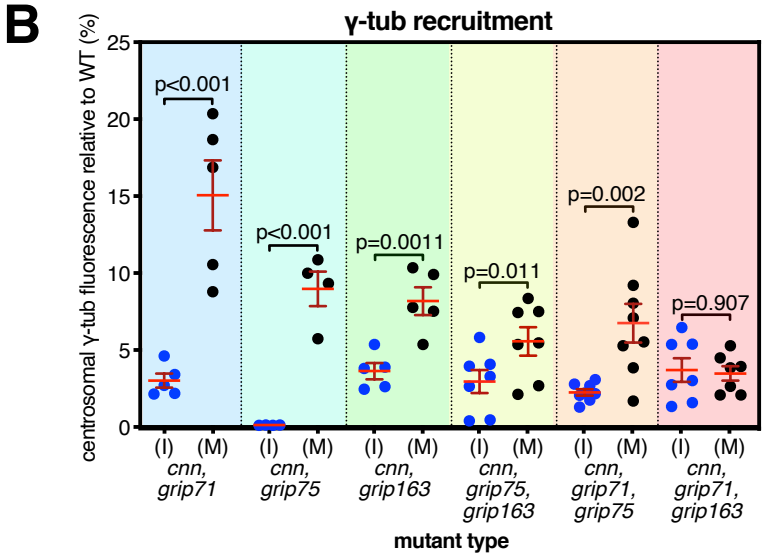
B
γ-tub recruitment
centrosomal γ-tub fluorescence relative to WT (%)
p<0.001
p<0.001
p=0.0011
p=0.011
p=0.002
p=0.907
(I) (M)
cnn, grip71
cnn, grip75
cnn, grip163
cnn, grip75, grip163
cnn, grip71, grip75
cnn, grip71, grip163
mutant type

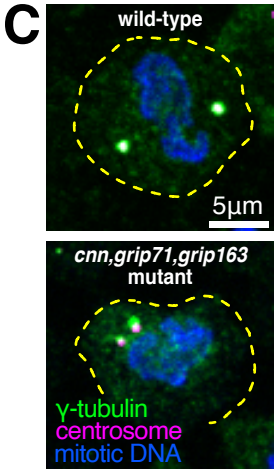
C
wild-type
5µm
cnn,grip71,grip163
mutant
γ-tubulin
centrosome
mitotic DNA

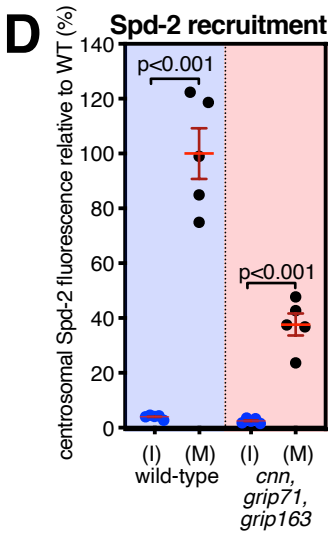
D
Spd-2 recruitment
centrosomal Spd-2 fluorescence relative to WT (%)
p<0.001
p<0.001
(I) (M)
wild-type
cnn, grip71, grip163

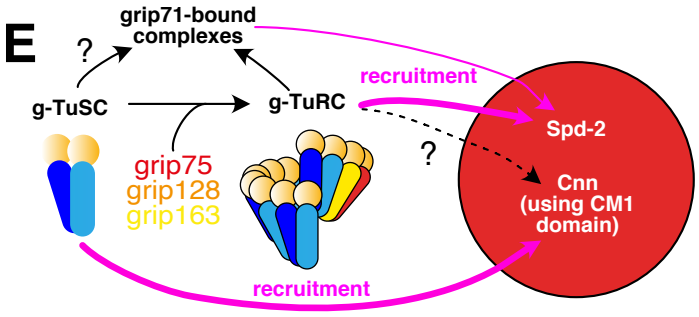
E
grip71-bound complexes
?
g-TuSC
g-TuRC
recruitment
Spd-2
grip75
grip128
grip163
?
Cnn (using CM1 domain)
recruitment

Figure 3

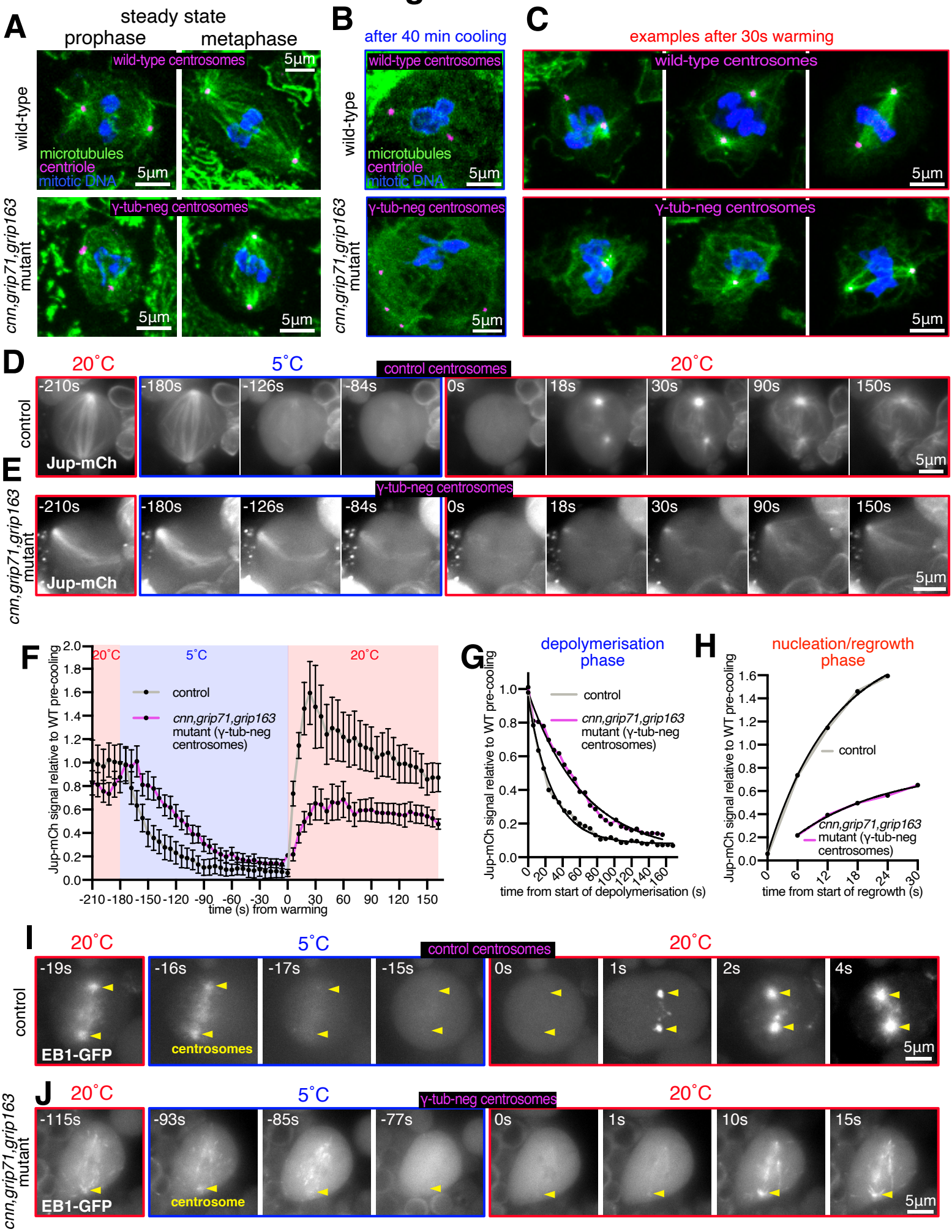
A
steady state
prophase
metaphase
wild-type
wild-type centrosomes
5µm
microtubules
centriole
mitotic DNA
5µm
cnn,grip71,grip163 mutant
γ-tub-neg centrosomes
5µm
5µm
B
after 40 min cooling
wild-type
wild-type centrosomes
microtubules
centriole
mitotic DNA
5µm
cnn,grip71,grip163 mutant
γ-tub-neg centrosomes
5µm
C
examples after 30s warming
wild-type centrosomes
5µm
γ-tub-neg centrosomes
5µm
D
20˚C
5˚C
control centrosomes
20˚C
control
-210s
-180s
-126s
-84s
0s
18s
30s
90s
150s
Jup-mCh
5µm
E
cnn,grip71,grip163 mutant
γ-tub-neg centrosomes
-210s
-180s
-126s
-84s
0s
18s
30s
90s
150s
Jup-mCh
5µm
F
20˚C
5˚C
20˚C
control
cnn,grip71,grip163 mutant (γ-tub-neg centrosomes)
Jup-mCh signal relative to WT pre-cooling
time (s) from warming
G
depolymerisation phase
control
cnn,grip71,grip163 mutant (γ-tub-neg centrosomes)
Jup-mCh signal relative to WT pre-cooling
time from start of depolymerisation (s)
H
nucleation/regrowth phase
control
cnn,grip71,grip163 mutant (γ-tub-neg centrosomes)
Jup-mCh signal relative to WT pre-cooling
time from start of regrowth (s)
I
20˚C
5˚C
control centrosomes
20˚C
control
-19s
-16s
-17s
-15s
0s
1s
2s
4s
EB1-GFP
centrosomes
5µm
J
20˚C
5˚C
γ-tub-neg centrosomes
20˚C
cnn,grip71,grip163 mutant
-115s
-93s
-85s
-77s
0s
1s
10s
15s
EB1-GFP
centrosome
5µm

Figure 4

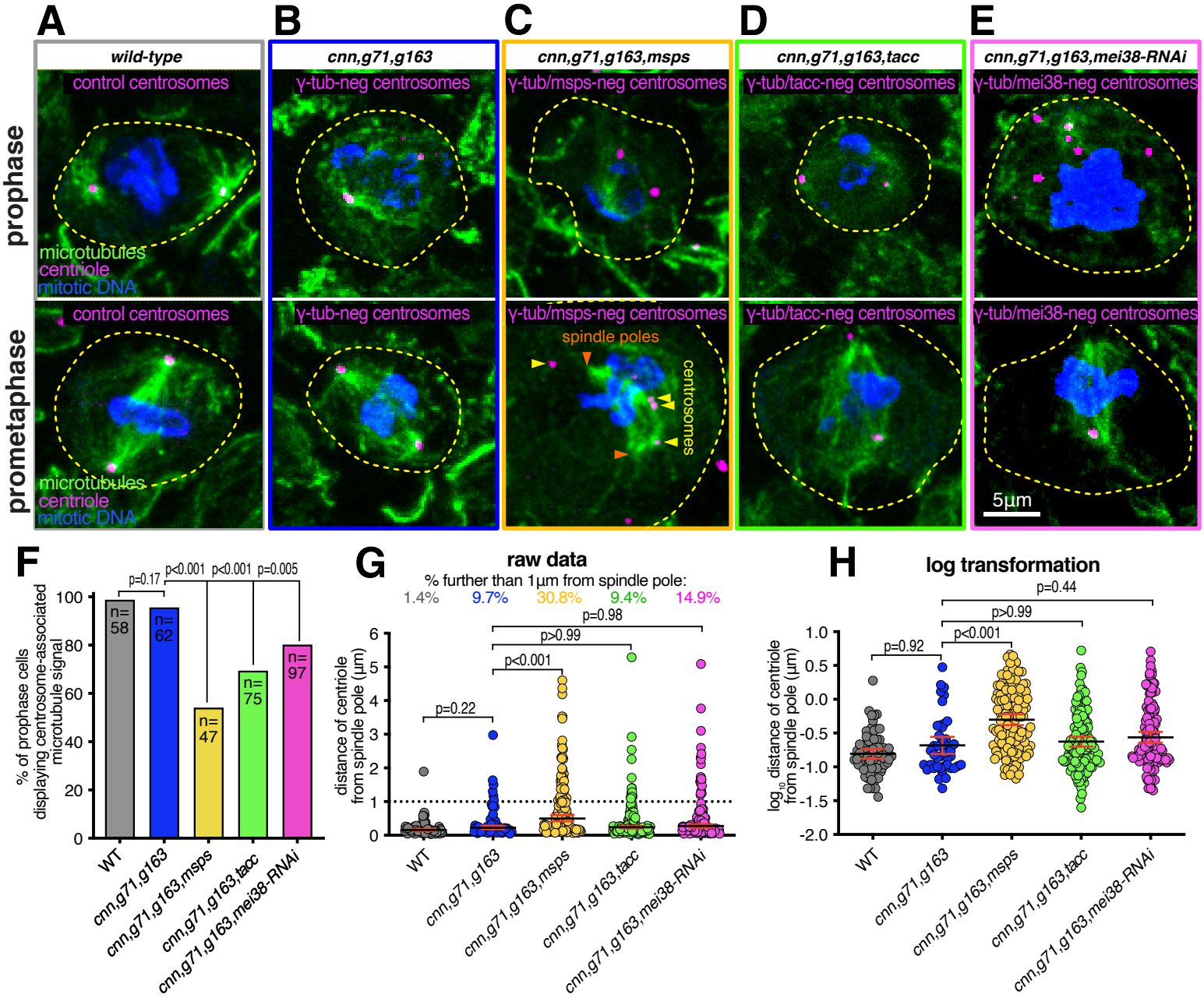
A
B
C
D
E
wild-type
cnn,g71,g163
cnn,g71,g163,msps
cnn,g71,g163,tacc
cnn,g71,g163,mei38-RNAi
prophase
prometaphase
control centrosomes
γ-tub-neg centrosomes
γ-tub/msps-neg centrosomes
γ-tub/tacc-neg centrosomes
γ-tub/mei38-neg centrosomes
microtubules
centriole
mitotic DNA
spindle poles
centrosomes
5µm
F
% of prophase cells displaying centrosome-associated microtubule signal
p=0.17
p<0.001
p<0.001
p=0.005
n= 58
n= 62
n= 47
n= 75
n= 97
WT
cnn,g71,g163
cnn,g71,g163,msps
cnn,g71,g163,tacc
cnn,g71,g163,mei38-RNAi
G
raw data
% further than 1µm from spindle pole:
1.4%
9.7%
30.8%
9.4%
14.9%
distance of centriole from spindle pole (µm)
p=0.22
p<0.001
p>0.99
p=0.98
H
log transformation
log10 distance of centriole from spindle pole (µm)
p=0.92
p<0.001
p>0.99
p=0.44

Figure 5

A **centrosome aster analysis** in cells yet to form spindle, 30s post warming

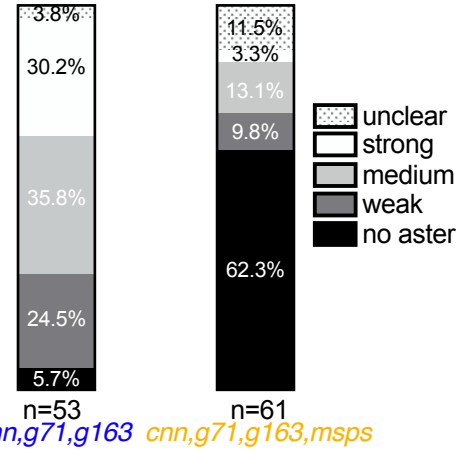

B cells yet to form spindle (30s post warming)

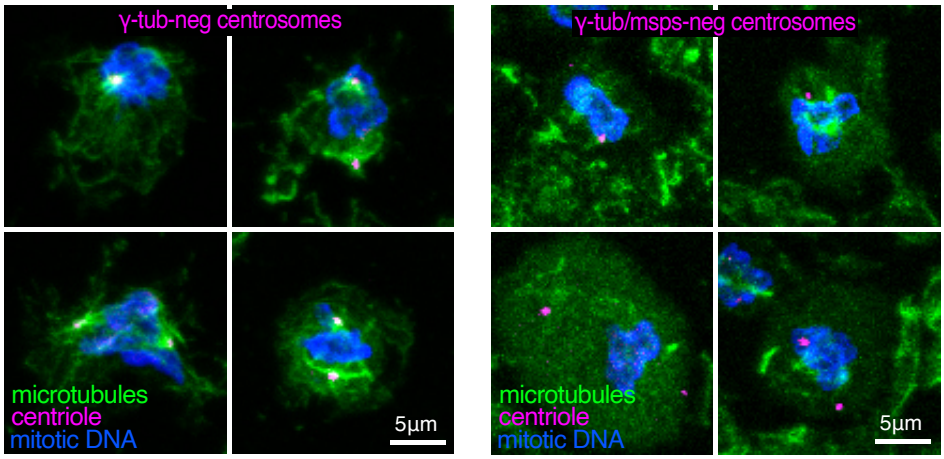

C **spindle quality analysis** in cells that had formed spindle and that contained centrosomes, 30s post warming

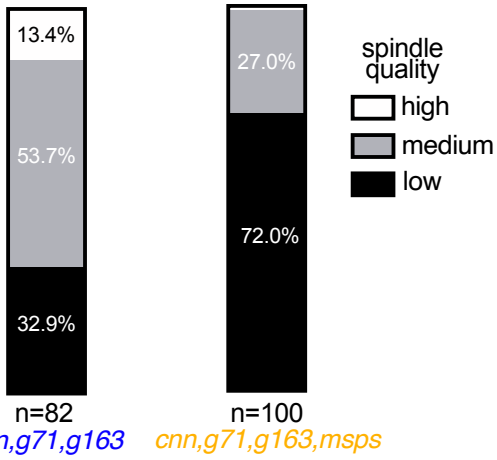

D cells that had formed spindle and that contained centrosomes (30s post warming)

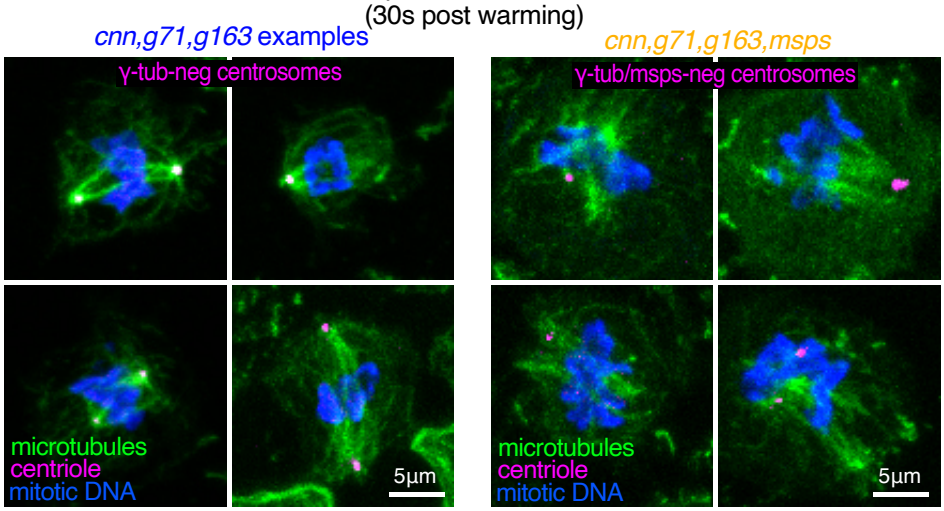

E **spindle quality analysis** in cells that had formed spindle and that lacked centrosomes, 30s post warming)

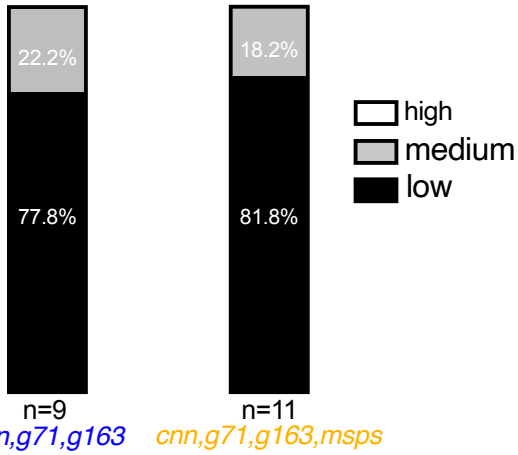

Figure S1

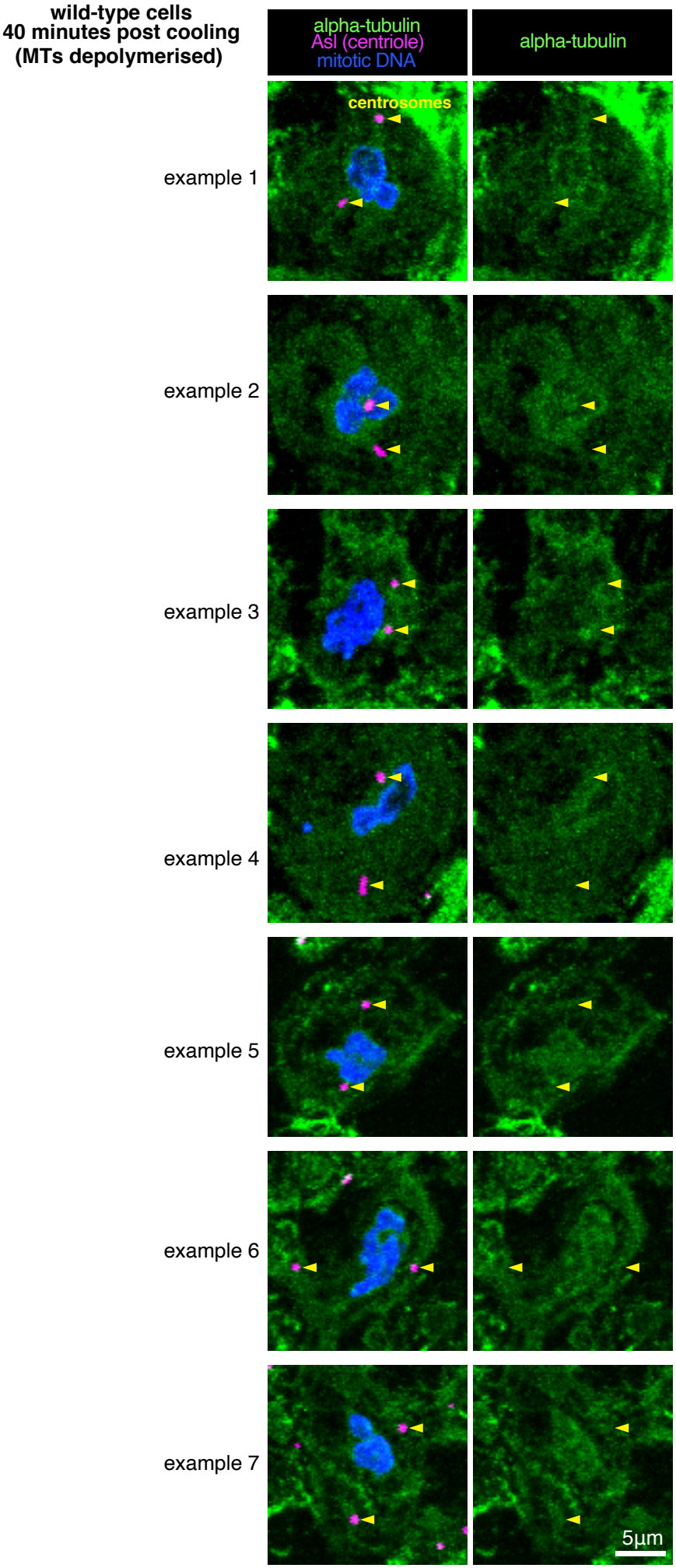
wild-type cells
40 minutes post cooling
(MTs depolymerised)
alpha-tubulin
Asl (centriole)
mitotic DNA
alpha-tubulin
centrosomes
example 1
example 2
example 3
example 4
example 5
example 6
example 7
5µm

Figure S2

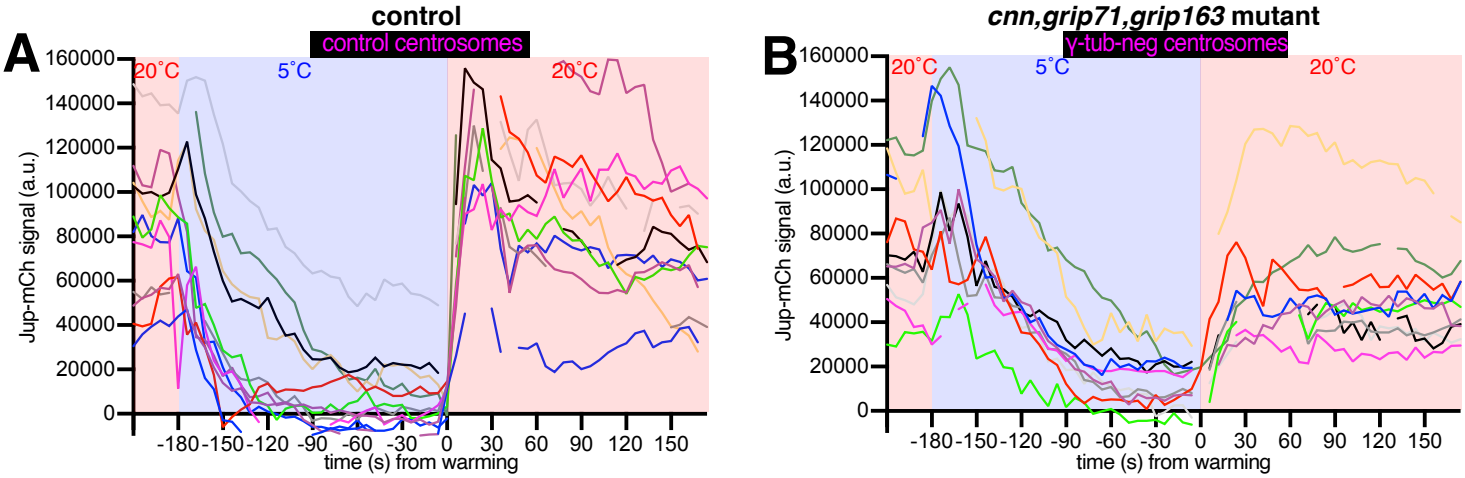
A
control
control centrosomes
20˚C
5˚C
20˚C
Jup-mCh signal (a.u.)
160000
140000
120000
100000
80000
60000
40000
20000
0
-180 -150 -120 -90 -60 -30 0 30 60 90 120 150
time (s) from warming
B
cnn,grip71,grip163 mutant
γ-tub-neg centrosomes
20˚C
5˚C
20˚C
Jup-mCh signal (a.u.)
160000
140000
120000
100000
80000
60000
40000
20000
0
-180 -150 -120 -90 -60 -30 0 30 60 90 120 150
time (s) from warming

Figure S3

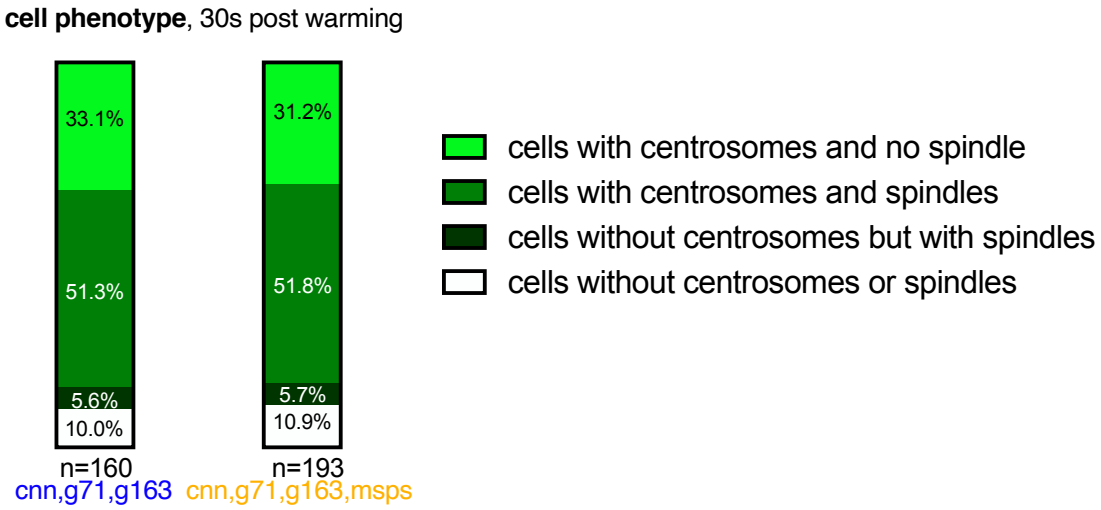
cell phenotype, 30s post warming
33.1%
51.3%
5.6%
10.0%
n=160
cnn,g71,g163
31.2%
51.8%
5.7%
10.9%
n=193
cnn,g71,g163,msps
cells with centrosomes and no spindle
cells with centrosomes and spindles
cells without centrosomes but with spindles
cells without centrosomes or spindles